A NUMERICAL STUDY ON SOLID PHASE TRANSFORMATION OF A PLAIN C-Mn STEEL

A thesis submitted in partial fulfilment of the requirements for the award of the degree of

Master of Engineering in Metallurgical Engineering

Faculty of Engineering and Technology
Jadavpur University

Submitted by

AMIT KUMAR HAZRA
Examination Roll No: M4MET24002
University Roll No: 002211302002
Registration No: 163719 of 2022-23

Under the Guidance of

Dr. Md. Basiruddin Sk.
Assistant Professor
Dept. of Metallurgical and Material Engineering
Jadavpur University, Kolkata-700032

Prof. Nilkanta Barman
Professor
Dept. of Mechanical Engineering
Jadavpur University, Kolkata-700032

DEPARTMENT OF METALLURGICAL AND MATERIAL ENGINEERING
FACULTY OF ENGINEERING AND TECHNOLOGY
JADAVPUR UNIVERSITY
KOLKATA

May 2024

DEDICATED

TO MY BELOVED FAMILY MEMBERS

CERTIFICATE

This is to certify that the thesis entitled "**A Numerical Study on Solid Phase Transformation of a Plain C-Mn Steel**" has been carried out by **Amit Kumar Hazra (Examination Roll No: M4MET24002, University Roll No: 002211302002 and Registration No: 163719 of 2022-23)** under our guidance and supervision and accepted in partial fulfilment for the degree of Master of Engineering in Metallurgical Engineering from the Department of Metallurgical and Material Engineering of Jadavpur University. To the best of our knowledge the content of this thesis or any parts thereof have not been previously submitted for the award of any degree.

……...
Supervisor
Dr. Md. Basiruddin Sk.
Assistant Professor
Department of Metallurgical and Material Engineering
Jadavpur University,
Kolkata-700032

……...
Co-Supervisor
Prof. Nilkanta Barman
Professor
Department of Mechanical Engineering
Jadavpur University,
Kolkata-700032

……...
Head of the Department
Dr. Sathi Banerjee
Department of Metallurgical and Material Engineering
Jadavpur University,
Kolkata-700032

……...
DEAN
Prof. Dipak Laha
Faculty of Engineering and Technology
Jadavpur University,
Kolkata-700032

DECLARATION OF ORIGINALITY AND COMPLIANCE OF ACADEMIC ETHICS

I hereby declare that this thesis "**A Numerical Study on Solid Phase Transformation of a Plain Carbon-Manganese Steel**" contains literature survey and original research work by me, as a part of my Master of Engineering Degree in Metallurgical Engineering during the academic year 2022-2024. All information in this document has been obtained and presented in accordance with academic rules and ethical conduct. I also declare that, as required by this rules and conduct, I have fully cited and referred all material and results that are not original to this work.

Name: Amit Kumar Hazra
Examination Roll No: M4MET24002
University Roll No: 002211302002
Registration No: 163719 of 2022-23

Thesis Title: **A Numerical Study on Solid Phase Transformation of a Plain Carbon-Manganese Steel**

Place: Kolkata
Date: Signature

CERTIFICATE OF APPROVAL

*The foregoing thesis, entitled as "**A Numerical Study on Solid Phase Transformation of a Plain Carbon-Manganese Steel**" is hereby approved by the committee of final examination for evaluation of the thesis as a creditable study of an engineering subject carried out and presented by **Amit Kumar Hazra (Examination Roll No: M4MET24002, University Roll No: 002211302002 and Registration No: 163719 of 2022-23)** in a manner satisfactory to warrant its acceptance as a prerequisite to the degree of Master of Engineering in Metallurgical Engineering. It is understood that by this approval, the undersigned do not necessarily endorse or approve any statement made, opinion expressed or conclusion drawn therein, but approve the thesis only for the purpose for which it is submitted.*

Committee of final examination for evaluation of thesis –

…… ……

…… ……

ACKNOWLEDGEMENT

I would like to take this opportunity to express my heartfelt gratitude to the people who supported me throughout this research project. I owe a deep sense of gratitude to my respected thesis supervisor(s) ***Dr. Md. Basiruddin Sk****, Assistant Professor, Department of Metallurgical and Material Engineering, Jadavpur University and* ***Prof. Nilkanta Barman****, Professor, Department of Mechanical Engineering, Jadavpur University for their esteemed guidance and encouragement throughout this work. Without their generous support and motivation this would not have been completed. It was a great privilege and experience to work under them.*

I am indebted to ***Dr. Sathi Banerjee****, Head of the Department of Metallurgical and Material Engineering, Jadavpur University and* ***Prof. Pravash Chandra Chakraborti****, former Head of the Department of Metallurgical and Material Engineering, Jadavpur University for the facilities and support during the course of investigation.*

I am also grateful to all the faculty members and Research Scholars of Department of Metallurgical and Material Engineering, Jadavpur University for their moral support, help and cooperation. In this regard, I also thank all of the Department of Metallurgical and Material Engineering, Jadavpur University for their constant support.

I am also grateful to all the faculty members and Research Scholars of Department of Mechanical Engineering, Jadavpur University for their moral support, help and cooperation. In this regard, I also thank all of the Department of Mechanical Engineering, Jadavpur University for their constant support and kind cooperation.

I also express my heartiest gratitude and acknowledgement to my parents and family members for being a constant source of continuous moral courage, support, blessings and aspiration in each synergy of life. Finally, I take this occasion to thank all my friends and classmates who helped me with their valuable suggestions.

*Above all, I thank the '****Almighty God****' for showering his blessings during the days of this work.*

Date: ……

Amit Kumar Hazra
Department of Metallurgical and Material Engineering
Jadavpur University, Kolkata-700032

CONTENTS

LIST OF FIGURES

LIST OF TABLES

ABBREVIATIONS

Abbreviation	*Full-Form*
BEM	Boundary Element Method
CFD	Computational Fluid Dynamics
CCT	Continuous Cooling Transformation
CHT	Continuous Heating Transformation
CV	Control Volume
DEM	Discrete Element Method
f	Weighting factor
FDM	Finite Difference Method
FEM	Finite Element Method
FVM	Finite Volume Method
JMAK	Johnson-Mehl-Avrami-Kolmogorov
LB	Lattice Boltzmann
PDE	Partial Differential Equation
PT	Phase Transformations
S	Volumetric Source Term
SEM	Structural Element Method
TDMA	Tri-Diagonal Matrix Algorithm
X	Transformed fraction of a phase

NOMENCLATURE

Symbols	***Description***	***Unit***
k	Thermal conductivity	W/m-℃
t	Time	s
CR	Cooling rate	℃/s
CT	Cooling time	s
C_p	Specific heat	J/kg-℃
HR	Heating rate	℃/s
T	Temperature	℃
α	Heating rate	℃/s
β	Cooling rate	℃/s
ρ	Density	kg/m^3
Subscripts		
amb	Ambient	
cooling	Cooling	
heating	Heating	
holding	Holding	
bu	bainite upper (0.1% transformation)	
bl	bainite lower (99.9% transformation)	
fu	ferrite upper (0.1% transformation)	
fl	ferrite lower (99.9% transformation)	
pu	pearlite upper (0.1% transformation)	
pl	pearlite lower (99.9% transformation)	

ABSTRACT

Study on solid phase transformation using a computational method includes numerical and mathematical modelling, has incited a lot of interest among the researchers across the globe due to its diverse and emerging applications in engineering. In addition, the advancement of materials in the recent decades has flourished, especially in case of steel due to its superior properties over the other materials and wide applications in every sector of the engineering. Such properties of the steel depend on the transformed phases during its cooling. In this context, there are several research works cited in the literature on solid transformation of phases mostly involve experimental investigations. In practice, a real time prediction of such transformation is necessary in order to control the properties of the steel, which is difficult in experimentation. Moreover, experimentation is very expensive in nature. This work, therefore, includes a numerical study on solid phase transformation of a plain C-Mn steel. It involves mathematical modelling of heat transfer, and subsequent development of a numerical code in the FORTRAN platform. The numerical code is developed based on the finite volume method (FVM) considering the Crank-Nicolson scheme for discretizing the governing equations. The subsequent solution of the finally obtained discretized simultaneous equations is performed on the basis of TDMA algorithm. Suitable boundary conditions are then considered in the present work to represent the cooling behaviour of the steel, phase transformation phenomena and evolution of the fraction of phases depending on the heating condition, holding time, and cooling condition of the material. In the model, the phase transformation is considered using the Avrami equation, which allows to calculate the fraction of transformation. Along with the transformed fraction, this work is also predicted the transformation time of each phase during cooling. The developed code is then validated with a previously cited literature. With a good agreement, this code is extended to predict the evolution of the phases during cooling of the plain C-Mn steel. Since cooling rate is a major process parameter to control the transformation of the phases, a parametric study is also included under different cooling rates.

Keywords: *Computational Fluid Dynamics, Solid Phase Transformation, Plain C-Mn Steel, Mathematical Modelling, Numerical Modelling, Discretization, Finite Volume Method, FORTRAN, TDMA, Ferrite, Bainite, Pearlite.*

CHAPTER – I

Introduction and Literature Review

1.1 Background

Advancement in the material engineering plays a vital role in driving the innovations. There are numerous metals and alloys, and their composites; those are under investigation in context to the advancement in their mechanical and metallurgical properties [1-5]. Among these materials, steel remains a backbone of the modern civilization, and ubiquitous in development of infrastructure, machineries etc. in the area of automotive, aerospace, construction, and energy sectors. Such wide use of the steel due to its reasonable cost and appropriate qualities opens an emerging area of research. It has been known from several literatures [1-6], that there is a growing demand on enhancing the performance of steel through its microstructural development in the recent decades. This technique leads tailoring the properties of steel by manipulating its internal structure at the microstructural level. Achieving the desired specific microstructures in the steel significantly impact on its mechanical properties such as strength, toughness, ductility etc. This unlocks a new possibility of using the steel in diverse applications such as in construction, pipeline, automotive, pressure vessel, naval and defence.

Now, the microstructure of steel is intricately influenced by the heating and cooling processes they undergo during various essential processes. Thus, choice of the heating and cooling cycle has a profound impact on the final microstructure, and consequently on the mechanical properties of the steel products. Therefore, prediction of a desirable microstructure under a suitable heating and cooling cycle has become a crucial research area to meet the specific demands of respective industrial application. By controlling the cooling rate and temperature during manufacturing, industrial operation processes, etc, it is possible to obtain desirable microstructures in the steel products [1-5,7-8]. The manipulative control of such microstructure happens in phase transformations. The phase transformation can be liquid-state phase transformation and solid phase transformation. In case of solid transformation of the steel, obtaining a desirable combination of the ferrite, pearlite, bainite and martensite phases or combination of the corresponding microstructure is possible by controlling the cooling rate within a specific range of temperature where, each phase is responsible to certain specific properties of the steel, which makes the material stronger, tougher, and high resistant to wear and fatigue, etc.

Now, a better understanding is obtained on formation of the phases in solid essentially affects the mechanical properties of a high-performance steel. In parallel, it is found that the plain C-Mn steel and allied alloys have improved ductility, weldability, formability etc. than

the other grades of steel [9-10]; accordingly, a plain C-Mn steel is chosen here to study its phase transformation. The idea of increasing its strength, ductility, toughness and other properties depends on the available phases in the steel, and the appropriate transformation is a challenge, leading to consideration of suitable heat treatment processes [11].

There are several literatures as presented in the section 1.2, reported on solid phase transformation of the steel during its heat treatment. The majority of the literature considered experimental investigation of heat transfer and formation of microstructure, and related factors those change microstructure in solid state of materials during processing. As found, the experimentation is expensive in nature and time consuming, and the real-time phase evolution is not possible during experimentation; other way, a real time monitoring is not possible in experimentation. Whereas, a real time evolution of the phase transformation is possible through a numerical analysis in coordination with experimentation. In this context, it is found that there are a few literatures those reported on the numerical modelling of phase transformation of steel. Thus, this work considers a detailed numerical study on the solid phase transformation of a plain C-Mn steel under varied cooling rates.

1.2 Literature Review

Heat transfer and related phase transformation of a material during cooling are very complex in nature. Thus, a preliminary understanding of such phase transformation is necessary and includes a thorough review of the available literature. Based on the availability, majority of the literature involves experimental as well as analytical investigation to model the heat transfer and phase transformation of various materials under different cooling rates, and also reported the effect of cooling rate on microstructure, effect of the thermo-mechanical treatment on microstructure etc. The present review of the literature is sub-divided, accordingly: sub-section 1.2.1 presents literature reported on the modelling of heat transfer, sub-section 1.2.2 presents literature reported on solid phase transformation of steel at different heating and cooling profiles, sub-section 1.2.3 presents literature focused on the evolution of the phases in phase transformation, and sub-section 1.2.4 presents literature reported on methods of mathematical modelling, numerical modelling and analysis.

1.2.1 Review related to the Modelling of Heat Transfer

In this sub-section, the review of some literature is presented. The mentioned literature mainly reported on modelling of heat transfer in different material processing. This helps in clear understanding of the heat transfer phenomena in material.

Peng *et al.* [12] presented a critical and detailed review on the theory and model development for the heat transfer during thermal processes of a material. They summarized and explained the influence of crucial factors on the temperature distribution.

Salcudean and Abdullah [13] presented a numerical model for the heat treatment process and its effect on the phase change associated with it. They presented the enthalpy and source-based semi-analytical approaches, and reported a comparison with experiment, and thereby, found a good agreement.

Choudhary *et al.* [14] developed a steady-state three-dimensional heat flow model based on the concept of artificial effective thermal conductivity. The model is generally applicable to handle a wide range of geometrical shapes.

Polidori *et al.* [15] presented modelling of heat transfer in presence of a thermal conductivity enhancer within the computational domain. The presence of thermal conductivity enhancer increases effective thermal conductivity, and hence corresponding heat transfer.

Liu *et al.* [16] numerically studied the micro-scale heat transfer using both the CFD and LB (Lattice Boltzmann) approaches. A good agreement is found between their results and to the available experimental correlations.

Sun *et al.* [17] established a three-dimensional numerical model to study heat transfer of 316L stainless steel. The results of the simulation agreed well with the experiments.

Oliveira *et al.* [18] presented linear inverse model to evaluate cooling of a material undergoing phase transformation. It is found that the linear inverse heat conduction problem is suitable in case of fast cooling condition.

Samanta *et al.* [19] numerically predicted the heatlines and isotherms during cooling of a hot moving steel plate in presence of single spray-water jet. It is found that a suitable heat transfer zone for solid phase transformation is obtained by studying heatline distributions in the computational domain. Parametric results revealed that the suitable heat transfer region increases as cooling rate and jet velocity increase, and decreases as plate velocity increases.

Mukherjee *et al.* [20] numerically predicted the heatlines and isotherms of a hot moving steel plate undergoing cooling process in presence of multiple spray-water jets. It is found that the thermally unaffected zone decreases upon increasing the convective heat transfer coefficient, and increases with increase in plate velocity.

1.2.2 Review related to The Effect of Heat Treatment on Solid Phase Transformation

In this sub-section, the review of some literature is presented. The mentioned literature mainly reported on the effect of heat treatment on solid phase transformation under different conditions and subsequent phase evaluation.

Barman *et al.* [21] numerically studied the phase transformation behaviour during cooling of a hot moving steel plate by impinging water jets on the surface of the plate. It is found that the austenite phase undergoes a phase transformation, and results a combination of ferrite, bainite and pearlite based on cooling condition.

Liu *et al.* [22] presented numerical and analytical methods for determining the kinetic parameters during phase transformation, through the compatible experimental data. A good agreement is found between the experimental data and numerical predictions.

Dong *et al.* [23] compared transformation mechanisms between normal and reverse phase transformation in medium Mn steel using thermodynamic and kinetic analysis. It is found that during the reverse phase transformation, a rapid formation of the austenite phase occurs.

Ilmola *et al.* [24] presented coupled heat transfer and phase transformation of dual-phase steel in coil cooling. A three-dimensional transient heat transfer finite element model is considered to determine phase transformation fraction. A good agreement between the phase transformation model and experimental data is found and verified under industrial conditions.

El-Fallah [25] examined an alloy capable of generating a bainitic structure through phase transformation, leading to the desired microstructure. It is found that during isothermal transformation temperatures, a good understanding of the material behaviour and its application is possible.

Serajzadeh [26] presented a mathematical model based on the finite element method to predict the temperature history and microstructural changes during cooling of steel. It is

found that the time-temperature measurements obtained from microstructural examinations are used to validate the modelling results.

Barman *et al.* [27] numerically predicted the thermal and the phase transformation behaviours during cooling of a hot moving steel plate under multi water jets. Parametric research on the distribution of phases is also considered. It is found that the austenite phase is transformed to ferrite, bainite and/or pearlite.

Quan *et al.* [28] studied the multi-phase transformation kinetics of ultra-high-strength steel and its application in thermal-mechanical-phase coupling simulation by finite element method (FEM). It is found from the microstructure examination that austenite is transformed to ferrite, pearlite, bainite, and martensite based on different transforming temperatures. A good agreement was found between the experimental and simulation results.

Villa *et al.* [29] investigated the aging of 17-4 PH martensitic stainless steel prior to hardening along with its effect on the martensitic phase transformations, evolution of microstructure and properties. It is found that mechanical properties of materials depend upon the austenite transformation, which attains a maximum strength in martensitic state.

Ghafouri *et al.* [30] presented the effect of solid phase transformation on deformations using comprehensive phase transformation modelling. It is found that the anisotropic conductivity agrees well with the experiments when temperature histories and thermocouples are compared.

Dai *et al.* [31] presented the application of solid phase transformations for advanced high strength steels containing metastable retained austenite. It is found that due to the extensive and step by step conduct of the work, it is beneficial to experts.

Rezaei *et al.* [32] presented the phase transformation kinetics of high-carbon steel during continuous heating. Study includes the effects of heating temperature, heating rate and holding time on the austenitization process of near-eutectoid high-carbon steel. It is found that the effect of heating rate on the austenitization process can be monitored by a continuous heating transformation (CHT) diagram. Based on the results, two distinct phase transition processes are revealed by the activation energy values.

Yamanaka [33] presented simulation of the solid phase transformations in iron and steel with recent advances in the phase-field modelling of the austenite-to-ferritic, pearlitic, bainitic, and martensitic transformations. It is found that evolution of microstructure during phase transformation can be predicted accurately by phase-field modelling.

Sun *et al.* [34] presented solid phase transformation to examine the variability in residual stresses in case of ferritic steel S355. It is found that keeping the solid phase transformation independent of strain hardening gives a higher degree of accuracy.

1.2.2.1 Review Related to Heating Effect on Solid Phase Transformation

In this sub-section of 1.2.2, the review of some literature is presented. The mentioned literature mainly reported on the heating effect on solid phase transformation of a material.

Razzak [35] presented heat treatment and the effects of Cr and Ni on phase transformation of low carbon steel. It is found that at temperatures below 975°C, chromium carbide refines less austenite in presence of nickel with accelerated phase transformations.

Sikander and Gangwar [36] presented the effects of austempering and martempering on microstructure and mechanical properties of EN31 steel. It is found that the mechanical properties depend on the retained austenite, bainite, ferrite, and carbide during austempering whereas properties during martempering are determined by retained martensite, bainite, and pearlite.

Krishna *et al.* [37] presented the effect of austempering and martempering on AISI 52100 steel. During heat treatment process, various tests are conducted for microstructural analysis. It is found that austempered steel has the highest strength, martempered steel is toughest and annealed steel is least hard post phase transformations.

Ataiwi and Betti [38] presented the microstructure and mechanical properties of high chromium white cast iron (HCWCI) under different martempering quenching mediums. It is found that the hardness increased while the toughness decreased.

Chen *et al.* [39] presented the influence of annealing on the microstructural and textural evolution of cold-rolled Er metal. It is found that the orientation of some planes is strengthened, while some planes have no improvement.

Rao *et al.* [40] presented the effect of annealing on the microstructure and mechanical properties of Al 6061 alloy. It is found that the microstructural properties enhanced as a result.

Qawabah *et al.* [41] presented the effect of annealing temperature on the microstructure, and mechanical behaviour of low carbon steel grade 45. It is found that the microstructural properties and the mechanical properties improves with increased annealing temperatures.

Szala *et al.* [42] presented the effects of annealing process parameters on the microstructure of $42CrMo_4$ steel by Finite element method (FEM) simulations. It is found that upon annealing, the microstructural properties improved while the hardness decreased.

1.2.2.2 Review Related to The Effect of Austenitization on Solid Phase Transformation

In this sub-section of 1.2.2, the review of some literature is presented. The mentioned literature mainly reported on the effect of austenitization on solid phase transformation of a material.

Liu *et al.* [43] presented the effect of batch annealing for different temperatures of an ultra-low carbon enamel steel. It is found that the ferrite grain expands and the other particles coarsens with increased annealing temperatures.

Basiruddin *et al.* [44] discussed how the impact transition behavior of steel bars that have undergone thermomechanical treatment is affected by the phases and textures. The best combination of strength, ductility, and impact toughness is found in higher section rebar. The impact toughness is influenced by the residual stress distribution inside the rebars.

Pan *et al.* [45] presented the effect of heat treatment under different conditions on a Fe-Si-Cr-Mo-C deep drawing dual-phase steel to improve the mechanical properties of steel. It is found that at modest rate of cooling martensite is produced, while at increased rate of cooling bainite and pearlite are produced.

Stoudt *et al.* [46] discussed how the annealing temperature affects the formation of different phases in the material. It is discovered that, in contrast to homogenized material, unhomogenized material significantly influences phase formation in a prominent way.

Simsir and Gur [47] presented a mathematical framework based on finite element method (FEM) capable of predicting temperature history, and evolution of phases during thermal treatment of metals and alloys. The simulation is justified by laboratory methods. It is found that the model accurately anticipates trends in the distribution of microstructures.

Wang *et al.* [48] presented an ultrafine-grained ultra strong high-carbon steel by heat treatment process. It is found that the microstructure consists of high carbon retained austenite and tempered martensite post phase transformations.

Poletti *et al.* [49] presented correlation between microstructural changes and thermodynamic parameters in low carbon steels. Result showed that the thermodynamic parameters have a significant influence on the microstructural changes.

Moniruzzaman *et al.* [50] presented heat treatment process for PH13-8Mo stainless steel by studying the kinetics of phase transformation, and microstructure evolution. It is found that different thermal profile results different microstructures and different thermo-mechanical properties.

1.2.2.3 Review related to Cooling Effect on Solid Phase Transformation

In this sub-section of 1.2.2, the review of some literature is presented. The mentioned literature mainly reported on the effect of cooling rate on the phase transformation of a material.

Karmakar *et al.* [51] presented the effects of cooling rate and steel composition on microstructures, precipitates and tensile properties. It is found that carbon content and an intermediate cooling rate about (~1.4 K/s) is very crucial for strengthening steel.

Ekinci *et al.* [52] presented the effects of heat treatment and cooling rate on the microstructure and mechanical properties of low-carbon microalloyed steels. It is found that variations in cooling rates and heat treatment impacts the microstructure and mechanical properties of steel.

Chen *et al.* [53] presented a new kind of low-carbon bainitic steel with excellent strength and toughness for application in various sectors by considering the effect of cooling rate on microstructure and mechanical properties. It is found from the thermal cycle that the specimen shows diverse fracture characteristics under increased and decreased cooling rates.

Barman *et al.* [54] analytically predicted the thermal behaviour of a hot steel strip cooled with water spray. The cooling process is represented by a steady state 2-D energy conservation equation. It is found that the analytical prediction makes a very good agreement with the numerical predictions.

Kozlowska *et al.* [55] presented the effects of heating and cooling rates on the microstructure of a double soaked medium-Mn 0.16C-5Mn-1.6Al-0.2Si steel with an increased Al addition. It is found that the microstructure is slightly impacted by variations in the applied heating and cooling rates whereas variations are observed in dilatometer upon cooling to room temperature.

Zheng *et al.* [56] presented experimental and numerical study of the cooling rates variation and its effect on the post-formed strength and phase evolutions of steel. It is found that higher temperatures and cooling rates promotes phase transformations. The experimental and numerical results agreed fairly.

Dey *et al.* [57] presented the effects of cooling rate and strain rate on the phase transformation, microstructure and mechanical behaviour of thermomechanically processed pearlitic steel. It is found that strain rate accelerates the pearlite transformation and ignition temperature of transformation.

Waimann and Reese [58] presented a variational material model that displays the phase transformations which occur during thermal processes. It is found that depending on the cooling rate, the model can depict the transformation between austenite and ferrite, austenite and martensite, or a combination of both. Calculations and finite element simulations agreed fairly proving its ability to deal with complex material behaviour.

Yang *et al.* [59] presented the influence of varying cooling rate on the microstructure, phase transformation and compressive properties of specific steel. It is found that increase in cooling rate increases the secondary phase volume fraction and with varying cooling rates, different combinations of α(Al) phases are formed.

1.2.3 Review related to Evolution of the Phases in Solid Phase Transformation

In this sub-section, the review of related literature is presented. The mentioned literature mainly reported on evolution of the phases in solid phase transformation.

Sinha *et al.* [60] presented effect of cooling rate on microstructural/phase evolution based on theoretical model. The predicted evolution of the microstructure matches well with the microstructure observed in the experiments.

Zhang *et al.* [61] reviewed development of thermal models in material processing to evaluate phases and related mechanical properties. The major influencing parameters are discussed in the review paper.

Rappaz [62] introduced the model of heat flow to evaluate phases in order to forecast microstructural properties at a wide range of process parameters. Experimental and simulation results are compared under a variety of process parameters.

Kundu *et al.* [63] presented a coupled heat transfer and phase transformation model to predict temperature distribution and fraction of phases transformed during cooling in case of a low carbon steel wire rod. The four phases. i.e., ferrite, bainite, pearlite, and tempered martensite are found in case of the thermo-mechanically treated (TMT) rebar.

Grong and Shercliff [64] reviewed on modelling for evolution of the phases in metals processing. The finite element analysis is used for microstructural/phase modelling; however, it is concluded that the "internal state variable" approach is good.

Niżnik and Pietrzyk [65] presented the numerical modelling on kinetics of phase transformation. The experimental and numerical predictions are compared, and found a good agreement.

Mitilzer *et al.* [66] presented industrial process models that rely on the empirical material parameters for phase evolution. The effect of important alloying elements on the grain growth, recrystallization, and phase transformation in case of steel is discussed.

Fachinotti *et al.* [67] presented a model for the evolution of phase in a material, specifically eutectoid steel. It is found that upon heat treatment, the diffusionless (martensitic) and competitive diffusive (pearlitic) phases change.

1.2.4 Review Related to Numerical and Mathematical Modelling

In this sub-section, the review of some literature is presented. The mentioned literature mainly reported on numerical analysis and mathematical modelling.

Thabet and Thabit [68] presented the use of computational fluid mechanics for solving complex engineering problems including phase identification and transformation fraction by various methods. They summarised the methods and reported the use of them as per requirements.

Raman *et al.* [69] presented the applications of computational fluid dynamics (CFD) in order to stimulate the phase transformations in solid by using free-stream flow, and interaction of the fluid (liquids and gases) with surfaces defined by boundary conditions. It is found that computational fluid dynamics (CFD) simulations predicted the phase transformations accurately.

Bakker *et al.* [70] presented an overview on the software of computational fluid dynamics (CFD) which is being used for the solution of complex problems, like evolution of microstructures, phase transformations, and heat transfer modelling. It is concluded that using mathematical approach and computational fluid dynamics simulations reduces the complexities of the problem and helps in real-time management of the problem.

1.2.4.1 Review related to Numerical Analysis

Gaur and Chouhan [71] presented the role of numerical analysis in mathematics and its ability to solve problems related to accuracy and real-time management. It is found that numerical analysis is a critical part of mathematics that develops efficient methods to obtain numerical solutions in complex problems of engineering.

Reddy [72] presented finite element method (FEM) for determining phase transformations and heat transfer in materials. It is found that certain methods like the Rayleigh Ritz method, weighted residual methods (Galekin, Petrov-Galekin, method of least squares, and collocation methods), and variational methods of approximation are used to determine the phase transformations and heat transfer in different materials.

Rao *et al.* [73] presented an overview on the applications of finite element method (FEM) for solving complex problems like heat transfer, evolutions of microstructure and phase transformations. It is found that numerical techniques like boundary element method (BEM), discrete element method (DEM), and structural element method (SEM) are used for more accurate and real-time monitoring of such complex problems.

Eymard *et al.* [74] presented an overview on use of finite volume method (FVM). It is found that the finite volume method (FVM) is used as a discretization technique for solving problems related to control volume and domain of space, time, and energy.

Harish and Ajay [75] presented the problems related to the discretization of the fluxes at each control volume's boundaries for material phase transformation. It is found that the numerical fluxes are conservative, and consistent which makes the complex problem solving much easier.

Polyanin *et al.* [76] presented the applications and accuracy of finite volume method (FVM) by solving partial differential equations (PDE's) for computational fluid dynamics (CFD) in determination of heating and cooling cycles for materials and microstructure changes.

It is found that accuracy of the heating and cooling cycles is improved by fine-tuning the mesh size used in the discretization process.

Yavuz and Ertugrul [77] numerically presented the cooling system performance and effectiveness in aluminium to determine the parameters affecting the performance by computational methods. It is found that numerical simulations are better than experimental predictions.

1.2.4.2 Review related to Discretization of Finite Volume Method

Wesseling [78] presented the methods for discretizing the Euler and Navier-Stokes equations in both compressible and incompressible forms in determining heat flows and cooling rates. It is found that the presented methods agreed fairly with the experimental results.

Feistauer *et al.* [79] presented computational methods for compressible flow where the discretization of fluxes at the control volume boundaries are achieved through the application of the finite difference technique/method (FDM) for determination of heating profile and phase evolutions in different materials. It is found that Taylor series expansions are fruitful for the computational methods in achieving the desired heating profile and phase evolutions.

Gomez *et al.* [80] presented computational modelling of solid-solid phase transformation problems. It is found that in contrast to experimental results the computational results are more accurate due to better understanding of interfacial phenomena and phase-field method.

Patankar [81] presented formulation of governing equation, discretization of governing equation based on finite volume method (FVM), solving linear simultaneous equation based on TDMA and SIMPLER algorithm considering staggered grid in case of fluid flow analysis under power law and Crank-Nicolson scheme. This work also considers finite volume method (FVM) for solving the governing equations.

1.3 Summary of the Literature Review

A thorough review of the relevant literature has been carried out to identify specific objectives of the present work. Characteristics of different phenomena such as heat transfer modelling, heating and cooling profiles, thermomechanical treatment, and their effect on phase transformation and formation of phases are reviewed mainly, as available in the literature in the form of experimental and numerical analysis. The following is the summary of related reviewed literature.

- The majority of the literature considered experimental investigation of heat transfer and formation of phases, and related factors those change the phase in solid state of materials during processing.
- Transformation consists of a combination of different phases, i.e, ferrite, bainite, pearlite, and martensite while transforming from the austenite phase under different cooling rate following continuous cooling processes or step wise cooling processes. Among all phases, it is found that obtaining of bainite and/or fine pearlite is very difficult, whereas ferrite phase is found almost in all conditions.
- Based on the formation of phases in the steel, a change in the mechanical and thermal properties is observed as a consequence of the phases present. Mechanical properties include tensile, hardness, creep, ductility, toughness, brittleness, fatigue, strength, stiffness, resilience, elasticity and plasticity, yield strength, fracture, wear resistance, strain energy, anisotropy etc. The thermal properties include heat capacity, thermal conductivity, thermal expansion, thermal stresses, thermal shock resistance, specific heat, thermal diffusivity etc.
- As found in the literature, experimentation is expensive in nature and time consuming, and a real-time phase evolution is not possible during experimentation, thus a real time monitoring is also not possible in experimentation.
- It is observed that there are a few related literatures those reported on the numerical and analytical predictions of solid phase transformation.
- In the numerical analysis, prediction of the real-time phase evolution is possible. It considers a set of suitable and desired boundary conditions for better accuracy and approximation. Thus, a synchronization of the numerical analysis with experimentation

is able to evaluate the real time phase transformation, thereby increases work ability to precisely prediction of the phases and decreases expenses of experimentation.

On consideration of all above-mentioned factors, a numerical analysis is considered in this present work to investigate the solid phase transformation of a plain C-Mn steel under different process parameters.

1.4 Objective of the Present Work

In context to the summary of literature review as mentioned in the section 1.3, this work is a consideration of a numerical analysis of solid phase transformation of a plain C-Mn steel in order to observe evolution of phases under different cooling rates and process parameters. The study mainly focuses on the effect of different cooling rates on phase transformation of the steel. The results will most likely open up new possibilities for processing and applying the materials in challenging and creative ways, advancing numerous industries around the world.

In context to the above, it is worth to mention that the traditional trial and error based experimental approaches have encountered many difficulties in order to understand the basics of phase transformation, and effect of cooling rate and other parameters on the transformation. Moreover, the real time evolution of phases is not possible during any experiment. This work, thus, considered a numerical analysis to study solid phase transformation under different cooling rates. The study involves:

(i) Consideration of a physical problem similar to an experiment.

(ii) Mathematical modelling of the continuous cooling transformation (CCT) diagram, for incorporation of suitable boundary conditions as per the heating and cooling profiles and other experimental situations.

(iii) Mathematical modelling of phase transformation for identification of phases, calculation of cooling rate and calculation of transformed phases.

(iv) Numerical modelling of the governing equations: discretization based on the Finite Volume Method (FVM), followed by solution of the obtained simultaneous equation based on TDMA algorithm.

(v) Development of a programming code on the FORTRAN platform.

(vi) Prediction of the results under different process parameters.

1.5 Layout of the Thesis

Chapter – II: Mathematical and Numerical Modelling

Chapter – III: Results and Discussion

Chapter – IV: Conclusion and Future Scope of The Work

1.6 Closure

The present chapter enlightened the introductory part of this work along with related literature review includes mainly on modelling of heat transfer, effect of heat treatment on solid phase transformation, heating effect on solid phase transformation, effect of austenitization on solid phase transformation, cooling effect on solid phase transformation, evolution of phases, and numerical and mathematical modelling. The objective of the work is then presented in details.

References

[1]. J. Gray, and M. Pontremoli, Metallurgical options for API 5L grades X65, X70 and X80 linepipe, *International Conference Pipe Technology*, *Italy*, 1987

[2]. G. J. Baczynski, J. J. Jonas, and L. E. Collins, The influence of rolling practice on notch toughness and texture development in high-strength line pipe, *Metallurgical and Materials Transactions A*, Vol. 30 (12), 1999, pp. 3045-3054

[3]. Y. M. Kim, S. K. Kim, Y. J. Lim, and J. N. Kim, Effect of Microstructure on the Yield Ratio and Low Temperature Toughness of Linepipe Steels, *ISIJ International*, Vol. 42 (12), 2002, pp. 1571-1577

[4]. Y. J. Chao, J. D. Ward, and R. G. Sands, Charpy impact energy, fracture toughness and ductile-brittle transition temperature of dual-phase 590 Steel, *Materials and Design*, Vol. 28 (2), 2007, pp. 551-557

[5]. Kim, Y. Min, H. Lee, and N. J. Kim, Transformation behaviour and microstructural characteristics of acicular ferrite in line pipe steels, *Materials Science and Engineering A*, Vol. 478 (1-2), 2008, pp. 361-370

[6]. S. Vaynman, D. Isheim, R. P. Kolli, S. P. Bhat, D. N. Seidman, and M. E. Fine, High strength low-carbon ferritic steel containing Cu-Fe-Ni-Al-Mn precipitates, *Metallurgical and Materials Transactions A: Physical Metallurgy and Materials Science*, Vol. 39 (2), 2008, pp. 363-373

[7]. Saray, Onur, A. Purcek, I. Karaman, and J. H. Maier, Impact toughness of ultrafine-grained interstitial-free steel, *Metallurgical and Materials Transactions A: Physical Metallurgy and Materials Science*, Vol. 43 (11), 2012, pp. 4320-4330

[8]. S. W. Thompson, Interrelationships between yield strength, low-temperature impact toughness, and microstructure in low-carbon, copper-precipitation-strengthened, high strength low-alloy plate steels, *Materials Science and Engineering A*, Vol. 711, 2018, pp. 424-433

[9]. E. Lincoln, The Procedure Handbook of Arc Welding, 13th Edition, Lincoln Electric Company, Ohio, 1994

[10]. T. Gladman, The Physical Metallurgy of Microalloyed Steels, 1st Edition, CRC Press, Florida, 2002

[11]. Pearce, and Ray, Process improvement through thermal profiling: the goal of thermal profiling is to always increase quality and reduce waste. Three case histories – covering powder coating, baking and solder reflow applications, *Process Heating*, 2005

[12]. Z. Peng, E. Doroodchi, and B. Moghtaderi, Heat Transfer Modelling in Discrete Element Method (DEM) based Simulations of Thermal Processes: Theory and Model Development, *Progress in Energy and Combustion Science*, Vol. 79, 2020, 100847

[13]. M. Salcudean, and Z. Abdullah, On the Numerical Modelling of Heat Transfer during Solidification Processes, *International Journal for Numerical Methods in Engineering*, Vol. 25 (2), 1988, pp. 445-473

[14]. S. K. Choudhary, D. Mazumdar, and A. Ghosh, Mathematical Modelling of Heat Transfer Phenomena in Continuous Casting of Steel, *ISIJ International*, Vol. 33 (7), 1993, pp. 764-774

[15]. G. Polidori, S. Fohanno, and C. T. Nguyen, A note on heat transfer modelling of Newtonian nanofluids in laminar free convection, *International Journal of Thermal Sciences*, Vol. 46, 2007, pp. 739-744

[16]. Y. Liu, J. Cui, Y. X. Jiang, and W. Z. Li, A numerical study on heat transfer performance of microchannels with different surface microstructures, *Journal of Applied Thermal Engineering*, Vol. 31, 2011, pp. 921-931

[17]. Z. Sun, W. Guo, and L. Li, Numerical modelling of heat transfer, mass transport and microstructure formation in a high deposition rate laser directed energy deposition process, *Journal of Additive Manufacturing*, Vol. 33, 2020, 101175

[18]. A. V. S. Oliveira, J. Teixeira, V. Schick, D. Maréchal, M. Gradeck and S. Denis, Using a linear inverse heat conduction model to estimate the boundary heat flux with a material undergoing phase transformation, *Applied Thermal Engineering*, Vol. 219, 2023, 119406

[19]. S. Samanta, S. Mukherjee, M. Dhar, S. Barman, N. Barman, A. Mukhopadhyay, and S. Sen, Heatline based thermal behaviour during cooling of a hot moving steel plate using single jet, *Applied Mechanics and Materials*, Vol. 592-594, 2014, pp. 1622-1626

[20]. S. Mukherjee, S. Samanta, M. Dhar, S. Barman, N. Barman, A. Mukhopadhyay, and S. Sen, Heatline based thermal behaviour during cooling of a hot moving steel plate using multiple jets, *Procedia Materials Science*, Vol. 5, 2014, pp. 2063-2068

[21]. S. Barman, N. Barman, A. Mukhopadhyay, and S. Sen, A Numerical Study on the Phase Transformation behaviour during Cooling of a Moving Plate, *Proceedings of the 21st National & 10th ISHMT-ASME Heat and Mass Transfer Conference*, *IIT Madras, India*, 2011

[22]. F. Liu, F. Sommer, C. Bos, and E. J. Mittemeijer, Analysis of solid-state phase transformation kinetics: models and recipes, *International Materials Reviews*, Vol. 52 (4), 2007, pp. 193-212

[23]. Y. Dong, L. Xiang, C. Zhu, Y. Du, Y. Xiong, X. Zhang, and L. Du, Analysis of phase transformation thermodynamics and kinetics and its relationship to structure-mechanical properties in a medium-Mn high strength steel, *Journals of Materials Research and Technology*, Vol. 27, 2023, pp. 5411-5423

[24]. J. Ilmola, A. Pohjonen, S. Koskenniska, O. Seppälä, O. Leinonen, J. Jokisaari, J. Pyykkönen, and J. Larkiola, Coupled heat transfer and phase transformations of dual-phase steel in coil cooling, *Materials Today Communications*, Vol. 26, 2021, 101973

[25]. G. M. A. M. El-Fallah, Dilatometric study of high silicon bainitic steels: Solid-state transformations, *Results in Materials*, Vol. 19, 2023, 100430

[26]. S. Serajzadeh, Modelling of temperature history and phase transformations during cooling of steel, *Journal of Materials Processing Technology*, Vol. 146, 2004, pp. 311-317

[27]. S. Barman, N. Barman, A. Mukhopadhyay, and S. Sen, Studies on the Phase Transformation during Cooling of a Hot Moving Steel Plate under Multi Water Jets, *Journal of Machining and Forming Technologies*, Vol. 5 (3/4), 2013, pp. 137-149

[28]. G. Z. Quan, Z. Y. Zhan, L. Zhang, D. S. Wu, G. C. Luo, and Y. F. Xia, A study on the multi-phase transformation kinetics of ultra-high-strength steel & application in thermal-mechanical-phase coupling simulation of hot stamping process, *Materials Science and Engineering A*, Vol. 673, 2016, pp. 24-38

[29]. M. Villa, F. B. Grumsen, F. Niessen, T. Dahmen, L. Cao, M. Reich, O. Kessler, X. Huang, and M. A. J. Somers, Aging 17-4 PH martensitic stainless steel prior to

hardening: effects on martensitic transformation, microstructure and properties, *Materialia*, Vol. 32, 2023, 101882

[30]. M. Ghafouri, J. Ahn, J. Mourujärvi, T. Björk, and J. Larkiola, Finite element simulation of welding distortions in ultra-high strength steel S960 MC including comprehensive thermal and solid-state phase transformation models, *Engineering Structures*, Vol. 219, 2020, 110804

[31]. Z. Dai, H. Chen, R. Ding, Q. Lu, C. Zhang, Z. Yang, and S. V. D. Zwaag, Fundamentals and application of solid-state phase transformations for advanced high strength steels containing metastable retained austenite, *Materials Science and Engineering R*, Vol. 143, 2021, 100590

[32]. J. Rezaei, M. H. Parsa, and H. Mirzadeh, Phase transformation kinetics of high-carbon steel during continuous heating, *Journal of Materials Research and Technology*, Vol. 27, 2023, pp. 2524-2537

[33]. A. Yamanaka, Phase-field modelling and simulation of solid-state phase transformations in steels, *ISIJ International*, Vol. 63 (3), 2023, pp. 395-406

[34]. J. Sun, J. Hensel, J. Klassen, T. N. Pagel, and K. Dilger, Solid-state phase transformation and strain hardening on the residual stresses in S355 steel weldments, *Journal of Materials Processing Tech.*, Vol. 265, 2019, pp. 173-184

[35]. M. A. Razzak, Heat treatment and effects of Cr and Ni in low alloy steel, *Bulletin of Materials Science*, Vol. 34 (7), 2011, pp. 1439-1445

[36]. Sikander, and S. Gangwar, Effect of Austempering and Martempering on Microstructure and Mechanical Properties of EN31 Steel, *International Journal of Research in Advent Technology*, Vol. 4 (4), 2016

[37]. P. V. Krishna, R. R. Srikant, M. Iqbal, and N. Sriram, Effect of Austempering and Martempering on the properties of AISI 52100 Steel, *ISRN Tribology*, Vol. 2013, 2012, 515484

[38]. A. H. Ataiwi, and Z. A. Betti, Study the Microstructure and Mechanical Properties of High Chromium White Cast Iron (HCWCI) under different Martempering Quenching Mediums, *Engineering and Technology Journal*, Vol. 37 (A) (4), 2019, pp. 112-119

[39]. S. Chen, Y. Wang, X. Zhang, J. Li, Z. Li, W. Yang, D. Wu, Z. Wang, D. Chen, and N. Mao, The Influence of Annealing on the Microstructural and Textural Evolution of Cold-Rolled Er Metal, *Materials*, Vol. 15 (24), 2022, 8848

[40]. P. N. Rao, D. Singh, and R. Jayaganthan, Effect of annealing on microstructure and mechanical properties of Al 6061 alloy processed by cryorolling, *Material Science and Technology*, Vol. 29 (1), 2013, pp. 76-82

[41]. S. M. A. Qawabah, N. Alshabatat, and U. F. Qawabeha, Effect of Annealing Temperature on the Microstructure, Microhardness, Mechanical Behaviour and Impact Toughness of Low Carbon Steel Grade 45, *International Journal of Engineering Research and Applications*, Vol. 2 (3), 2012, pp. 1550-1553

[42]. M. Szala, G. Winiarski, L. Wojcik, and T. Bulzak, Effect of Annealing Time and Temperature Parameters on the Microstructure, Hardness, and Strain-Hardening Coefficients of 42CrMo$_4$ Steel, *Materials*, Vol. 13 (9), 2020, 2022

[43]. Z. Lui, Y. Kang, Z. Zhang, and X. Shao, Effect of Batch Annealing Temperature on Microstructure and Resistance to Fish Scaling of Ultra-Low Carbon Enamel Steel, *Metals*, Vol. 7 (2), 2017, 51

[44]. M. B. Sk, A. K. Khan, S. Lenka, B. Syed, J. Chakraborty, D. Chakrabarti, A. Deb, S. Chandra, and S. Kundu, Effect of Microstructure and Texture on the Impact Transition Behaviour of Thermo-mechanically Treated Reinforcement Steel Bars, *Materials and Design*, Vol. 90, 2016, pp. 1136-1150

[45]. H. Pan, X. Shen, D. Li, Y. Liu, J. Cao, Y. Tian, H. Zhan, H. Wang, Z. Wang, and Y. Xiao, Effect of Annealing Process on Microstructure, Texture, and Mechanical Properties of a Fe-Si-Cr-Mo-C Deep Drawing Dual-Phase Steel, *Crystals*, Vol. 10, 2020, 777

[46]. M. R. Stoudt, E. A. Lass, D. S. NG, M. E. Williams, F. Zhang, C. E. Campbell, G. Lindwall, and L. E. Levine, The Influence of Annealing Temperature and Time on the Formation of δ-Phase in Additively-Manufactured Inconel 625, *Metallurgical and Materials Transactions A*, Vol. 49 (A), 2018, pp. 3028-3037

[47]. C. Simsir, and C. H. Gur, A FEM based framework for simulation of thermal treatments: Application to steel quenching, *Computational Materials Science*, Vol. 44, 2008, pp. 588-600

[48]. J. Wang, Q. Tao, J. Fan, L. Fu, and A. Shan, Enhanced mechanical properties of a high-carbon martensite steel processed by heavy warm rolling and tempering, *Material Science and Engineering A*, Vol. 872, 2023, 144958

[49]. C. Poletti, F. Warchomicka, M. Dikovits, and S. Groβeiber, Microstructure evolution of allotropic materials during thermomechanical processing, *Material Science Forum*, Vol. 710, 2012, pp. 93-100

[50]. F. M. Moniruzzaman, S. I. Shakil, S. K. Shaha, J. Kacher, A. Nasiri, M. Haghshenas, and A. Hadadzadeh, Study of direct aging heat treatment of additively manufactured PH13-8Mo stainless steel: role of the manufacturing process, phase transformation kinetics, and microstructure evolution, *Journal of Materials Research and Technology*, Vol. 24, 2023, pp. 3772-3787

[51]. A. Karmakar, P. Sahu, S. Neogy, D. Chakrabarti, R. Mitra, S. Mukherjee, and S. Kundu, Effect of Cooling Rate and Chemical Composition on Microstructure and Properties of Naturally Cooled Vanadium-Microalloyed Steels, *Metallurgical and Materials Transactions A*, Vol. 48, 2017, pp. 1581-1595

[52]. C. Ekinci, N. Ucar, A. Calik, S. Karakas, and I. Akkurt, Effects of Heat Treatment on the Microstructure and Mechanical Properties of Low-Carbon Microalloyed Steels, *High Temperature Material Processing*, Vol. 30, 2011, pp. 39-42

[53]. J. Chen, Z. Zhang, Z. Zhang, Y. Liu, X. Zhao, J. Chen, and H. Chen, Effect of the Cooling Rate of Thermal Simulation on the Microstructure and Mechanical Properties of Low-Carbon Bainite Steel by Laser-Arc Hybrid Welding, *Coatings*, Vol. 12 (8), 2022, 1045

[54]. S. Barman, N. Barman, A. Mukhopadhyay, and S. Sen, Analytical Prediction of Thermal Behaviour during Cooling of a Hot Steel Strip, *Advanced Materials Research*, Vol. 585, 2012, pp. 19-23

[55]. A. Kozlowska, M. Morawiec, R. H. Petrov, and A. Grajcar, Effect of Heating and Cooling Rates on the Microstructure of a Double Soaked Medium-manganese Al-alloyed Steel, *Berg Huettenmaenn Monatsh*, Vol. 167 (11), 2022, pp. 538-541

[56]. K. Zheng, D. Li, H. Chen, S. Qu, Z. Zhao, Y. Zhang, and Y. Li, Effect of cooling rate on the phase transformation and post strength of Ti-6Al-4V under hot forming

conditions: Experiments and modelling, *Journal of Alloys and Compounds*, Vol. 972, 2024, 172868

[57]. I. Dey, S. K. Ghosh, and R. Saha, Effects of cooling rate and strain rate on the phase transformation, microstructure and mechanical behaviour of thermomechanically processed pearlitic steel, *Journal of Materials Research and Technology*, Vol. 8 (3), 2019, pp. 2685-2698

[58]. J. Waimann, and S. Reese, Variational modeling of temperature induced and cooling-rate dependent phase transformations in polycrystalline steel, *Mechanics of Materials*, Vol. 170, 2022, 104299

[59]. Q. Yang, W. Shi, M. Wang, L. Jia, W. Wang, and H. Zhang, Influence of cooling rate on the microstructure and mechanical properties of Al-Cu-Li-Mg-Zn alloy, *Journal of Materials Research and Technology*, Vol. 25, 2023, pp. 3151-3166

[60]. V. K. Sinha, R. S. Prasad, A. Mandal, and J. Maity, A Mathematical Model to Predict Microstructure of Heat-Treated Steel, *Journal of Materials Engineering and Performance*, Vol. 16 (4), 2007, pp. 461-469

[61]. Z. Zhang, Y. Wang, P. Ge, and T. Wu, A Review on Modelling and Simulation of Laser Additive Manufacturing: Heat Transfer, Microstructure Evolutions and Mechanical Properties, *Coatings*, Vol. 12, 2022, pp. 1277-1303

[62]. M. Rappaz, Modelling of microstructure formation in solidification process, *International Materials Reviews*, Vol. 34 (3), 1989, pp. 93-123

[63]. S. Kundu, A. Mukhopadhyay, S. Chatterjee, and S. Chandra, Modelling of Microstructure and Heat Transfer during Controlled Cooling of Low Carbon Wire Rod, *ISIJ International*, Vol. 44 (7), 2004, pp. 1217-1223

[64]. Ø. Grong, and H. R. Shercliff, Microstructural modelling in metals processing, *Progress in Material Science*, Vol. 47, 2002, pp. 163-282

[65]. B. Niżnik, and M. Pietrzyk, Model of phase transformation for niobium microalloyed steels, *Archives of Metallurgy and Materials*, Vol. 56 (3), 2011, pp. 731-742

[66]. M. Mitilzer, J. J. Hoyt, N. Provatas, J. Rottler, C. W. Sinclair, and H. S. Zurob, Multiscale Modelling of Phase Transformations in Steels, *The Minerals, Metals and Materials Society*, Vol. 66 (5), 2014, pp. 740-746

[67]. V. D. Fachinotti, A. Cardona, and A. A. Anca, Solid-State Microstructure Evolution in Steels, *Mecánica Computacional*, Vol. 994, 2005, pp. 901-914

[68]. S. Thabet, and T. H. Thabit, Computational Fluid Dynamics: Science of the Future, *International Journal of Research and Engineering*, Vol. 5 (6), 2018, pp. 430-433

[69]. R. K. Raman, Y. Dewang, and J. Raghuwanshi, A review on applications of computational fluid dynamics, *International Journal of LNCT*, Vol. 2 (6), 2018, pp. 137-143

[70]. A. Bakker, A. Haidari, and L. Oshinowo, Realize greater benefits from CFD, *Chemical Engineering Progress*, Vol. 97 (3), 2001, pp. 45-53

[71]. M. Gaur, and A. S. Chouhan, Current Role of Numerical Analysis in Mathematics, *International Journal for Modern Trends in Science and Technology*, Vol. 8 (06), 2022, pp. 412-418

[72]. J. N. Reddy, An Introduction to the Finite Element Method, 3rd Edition, McGraw-Hill Education, New York State, 2017

[73]. A. Rao, R. Khanna, and M. Gangopadhyay, Applications of Finite Elements Method (FEM)-An Overview, *International Conference on Mathematical Sciences*, *India*, 2012

[74]. R. Eymard, Herbin, and T. Gallouet, Finite volume method, Techniques of Scientific Computing, Part III, *Handbook of Numerical Analysis VII*, 2010, pp. 713-1020

[75]. Harish, and Ajay, Finite Element Method – FEM and FEA Explained, *Simscale*, 2019

[76]. A.D. Polyanin, W.E. Schiesser, and A.I. Zhurov, Partial Differential Equation, *Scholarpedia*, Vol. 3 (10), 2008, 4605

[77]. H. Yavuz, and O. Ertugral, Numerical Analysis of the Cooling System Performance and Effectiveness in Aluminium Low-Pressure Die Casting, *International Journal of Metalcasting*, Vol. 15 (1), 2021, pp. 216-228

[78]. P. Wesseling, Principles of computational fluid dynamics, *Springer Series in Computational Mathematics (SSCM)*, Vol. 29, Springer Publishing Company, New York, 2001

[79]. M. Feistauer, J. Felcman, and I. Straskraba, Mathematical and computational methods for compressible flow, *Numerical Mathematics and Scientific Computation*, Oxford Science Publications, Oxford, 2003

[80]. H. Gomez, M. Bures, and A. Moure, A review on computational modelling of phase-transition problems, *Phil. Trans. R. Soc. A*, Vol. 377, 2019, 20180203

[81]. S. V. Patankar, Numerical Heat Transfer and Fluid Flow, 1st Edition, CRC Press, New York, 1980

CHAPTER – II

Mathematical and Numerical Modelling

2.1 Introduction

The real-time evolution of phase transformation of steel is becoming increasingly challenging. It determines the metallurgical and mechanical properties of the steel. Such real-time evolution is a challenge to the researchers. Such phase transformation depends on several process parameters such as initial temperature, heating rate, holding temperature, holding time, cooling rate etc. Based on consideration of suitable process parameters, austenite phase of the steel transforms into a combination of ferrite, bainite, pearlite, and martensite during cooling. Trial and error basis experimental prediction is very expensive in nature, real-time monitoring is also difficult, and time consuming. Accordingly, this work considers a numerical analysis in order to predict the real-time phase transformation of a plain C-Mn steel, which is widely being used in engineering applications, under various process parameters. A suitable heat transfer model with appropriate boundary conditions is considered to evaluate the temperature distribution under desired heating and cooling profiles of the steel. A suitable model of the continuous cooling transformation (CCT) diagram of the steel and Avrami equation are considered for identification of the phases and their fractional transformation, respectively. Then the finite volume method (FVM) is considered to discretize the governing equation based on Crank-Nicolson scheme, and Tri-diagonal-matrix-algorithm (TDMA) is used to solve the obtained simultaneous linear equations. Thereafter, a numerical code is developed on the FORTRAN platform in order to predict the phases transformed during cooling of the plain C-Mn steel under different process parameters, includes a necessary validation of the developed code.

2.2 Description of the Physical Problem

This work considers a study on solid phase transformation of a material (as a specimen) under controlled heating and cooling conditions. In this context, a furnace with a temperature control unit is considered in order to control the temperature of the specimen. The specimen is of the plain C-Mn steel, considered here for its solid phase transformation. Fig. 2.1(a) represents a schematic of the controlled temperature furnace where the specimen is placed on its basement. In context to the above stated condition, a computational domain for the specimen is considered and shown in Fig. 2.1(b) with appropriate boundary conditions.

A usual furnace has different options to control its temperature with time such as isothermal heating, isothermal cooling, continuous cooling, etc. This work is considered a

temperature profile similar to the work reported by Karmakar *et al*. [84] as shown in the Fig. 2.2. The specimen initially is at an ambient temperature (T_{amb}), which is heated at a heating rate (α) for a period of $t_{heating}$. The specimen is maintained isothermally at $T_{holding}$ for a period of $t_{holding}$, and then cooled at a cooling rate (β) for transforming the phases. The necessary parameters in order to control the temperature of the furnace in the present case is tabulated in Table.2.1.

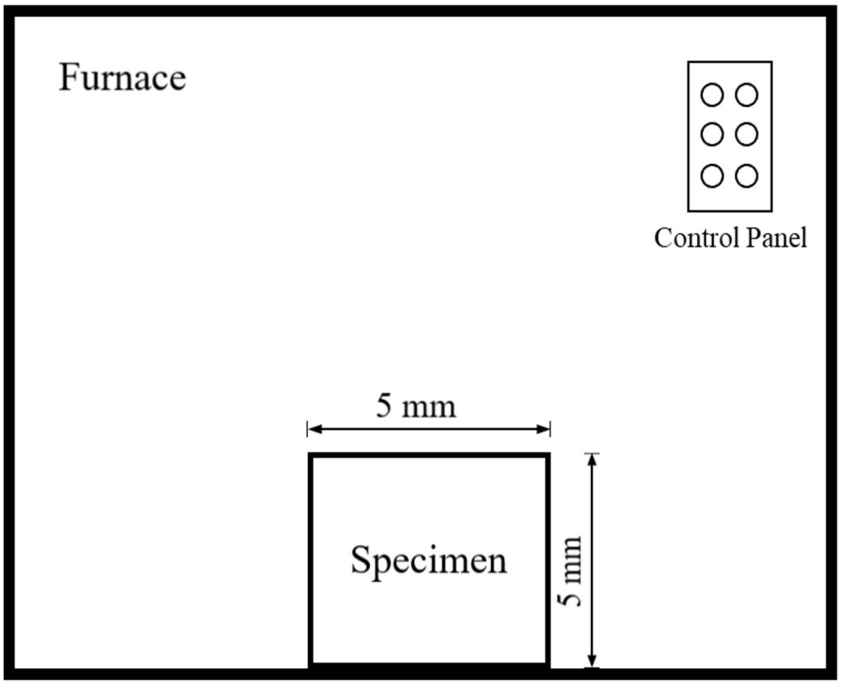

(a)

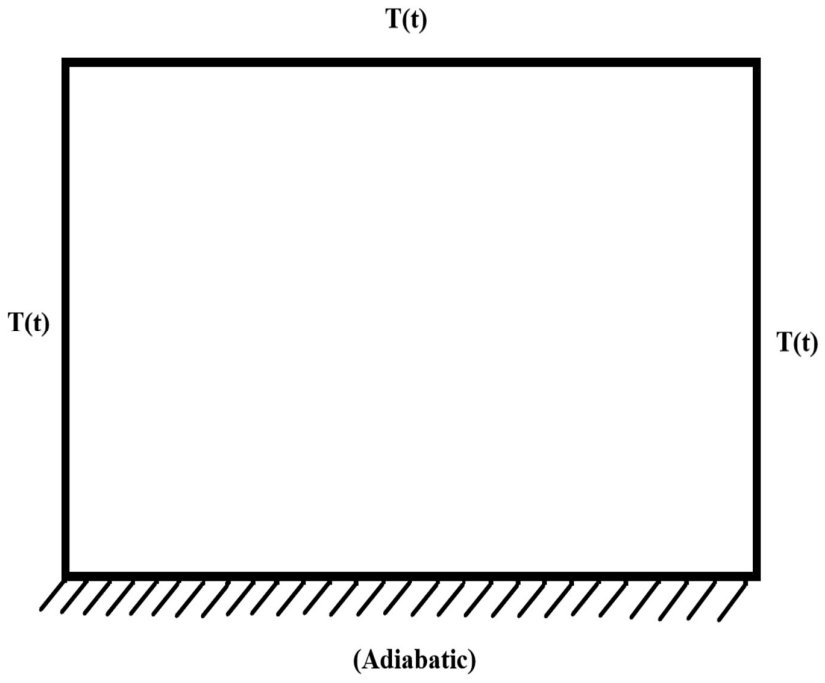

(b)

Figure 2.1: (a) Schematic of a controlled heating and cooling furnace with a specimen of plain C-Mn steel, and **(b)** schematic of a computational domain for the specimen of plain C-Mn steel

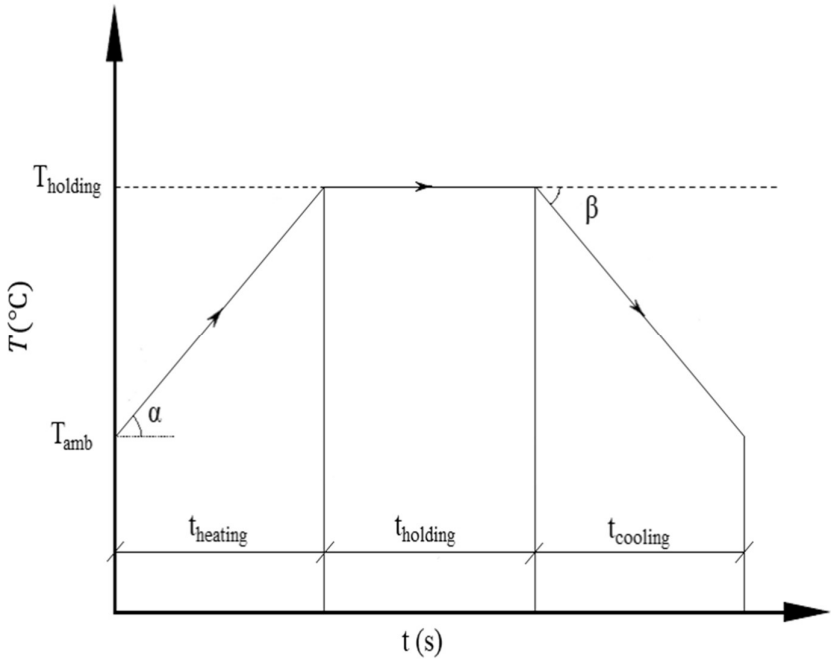

Figure 2.2: Variation of the furnace temperature with time

Table 2.1: Parameters related to the furnace temperature

Controlled Parameters	***Value***
Heating time (s)	3600
Holding time (s)	1800
Heating rate $(℃/s)$	0.345
Ambient temperature $(℃)$	28
Holding temperature $(℃)$	1100

2.2.1 Reasons behind consideration of the plain C-Mn steel

A proper choice of the material and its dimensions play vital role in order to achieve the objectives of the work. Accordingly, a plain C-Mn steel is considered in this work with the alloying chemical compositions as shown in the Table.2.2. Among various available alloys, the plain C-Mn steel is a profound and mutual choice by the researchers in the recent decades due to its advantageous properties over the other materials (Tian *et al.* [82]). The plain C-Mn steel has a simplified CCT diagram, as presented in the section 2.2.1.1 in details, where identification of the phases based on cooling rate is approximately possible and hence, the evolution of phases during cooling is also possible (Jeong *et al.* [83]).

Further, this material has following advantages over the others:

- **Properties:** It exhibits good mechanical, thermal and metallurgical properties which include good machinability and weldability, suitable strength, good ductility and toughness, recyclable, good thermal conductivity, specific heat capacity, etc. (Tian *et al*. [82]; Jeong *et al*. [83]). The necessary thermo-physical properties of the plain C-Mn steel is presented in the Table.2.3.
- **Availability:** It is readily available in various forms and sizes. Providing the easy access to the material for experimentations and testing (Tian *et al*. [82]).
- **Cost-effectiveness:** It is more affordable as compared to other steels. Therefore, it is a choice for various research investigations (Jeong *et al*. [83]).

- **Wide Applications:** It has a wide range of industrial and research applications including sectors like automobile industry, aerospace industry, structural component industries, mining and heavy machinery, defense sector, and emerging medical prosthetics. This leads a systematic study towards advancement of the material.

Table 2.2: Alloying Chemical Compositions of the Plain C-Mn Steel (Karmakar *et al*. [84])

	C	***Mn***	***Si***	***S***	***P***	***V***	***N***
Plain C-Mn	0.06	1.67	0.05	0.005	0.018	-	0.008

Table 2.3: Thermo-physical Properties of the Plain C-Mn Steel

Description of the properties	***Plain C-Mn Steel***
Density $(\boldsymbol{\rho, kg/m^3})$	7.85×10^3
Specific heat $(\boldsymbol{C_p, J/kg}.℃)$	570
Thermal conductivity $(\boldsymbol{k,\ W/m}.℃)$	53

2.2.1.1 Continuous Cooling Transformation (CCT) diagram of the Plain C-Mn Steel

A Continuous Cooling Transformation (CCT) diagram measures the extent of transformation as a function of time for a continuously decreasing temperature. It plays a crucial role in understanding the behaviour of a material during cooling. During phase transformation, valuable intricates are provided by the CCT diagram (Trzaska *et al.* [85]). Phase transformation

during cooling is illustrated depicting the beginning and end times of a particular phase. Under different conditions, austenite (the high-temperature phase in case of steel) transforms to different phases. Prediction of such formation of the phases (ferrite, pearlite, bainite, and martensite in case of steel) is attributed by the CCT diagram (Martin *et al.* [86]). In CCT diagram, the cooling curve is presented as variation of temperature with time, its slope indicates the formation of different phases. The fraction of such transformed phases is usually estimated by Avrami equation (Halmešová *et al.* [87]). By understanding the transformation behaviour of a material, a suitable advancement of the material is possible with specific heating and cooling profiles. This is being applied in the recent decades in order to achieve the desired material properties. Hence, prediction of the phase change based on the cooling rates and CCT diagram is essential for the material development. In this way, the CCT diagram helps to estimate the mechanical properties such as strength, ductility, and workability after thermal treatment of a material (Schindler *et al.* [88]).

Fig.2.3 is a continuous cooling transformation (CCT) diagram of plain C-Mn steel under different cooling rates. This CCT diagram is obtained using the JMatPro Software where the alloying compositions of the plain C-Mn steel are provided as input, and subsequent CCT diagram is obtained as the Fig.2.3.

In the Fig.2.3, different cooling rates such as 0.1℃/s, 1.0℃/s, 10℃/s, and 100℃/s are presented. A high temperature range upto 1100℃ is considered where the plain C-Mn steel is in austenite phase. During cooling under different cooling rate conditions, the ferrite phase begins to transform after the black curve (represented as ∗) near about 800℃. The ferrite phase continues its transformation. After attaining a certain temperature near about 600℃, based on the cooling rates, austenite transforms to either bainite or pearlite or their combination. The curve of light blue line (indicated as □) represents the start of bainitic transformation and the deep blue line (indicated as □) represents the end of bainitic transformation. The curve of light green line (indicated as □) represents the start of pearlitic transformation and the deep green line (indicated as o) represents the end pearlitic transformation

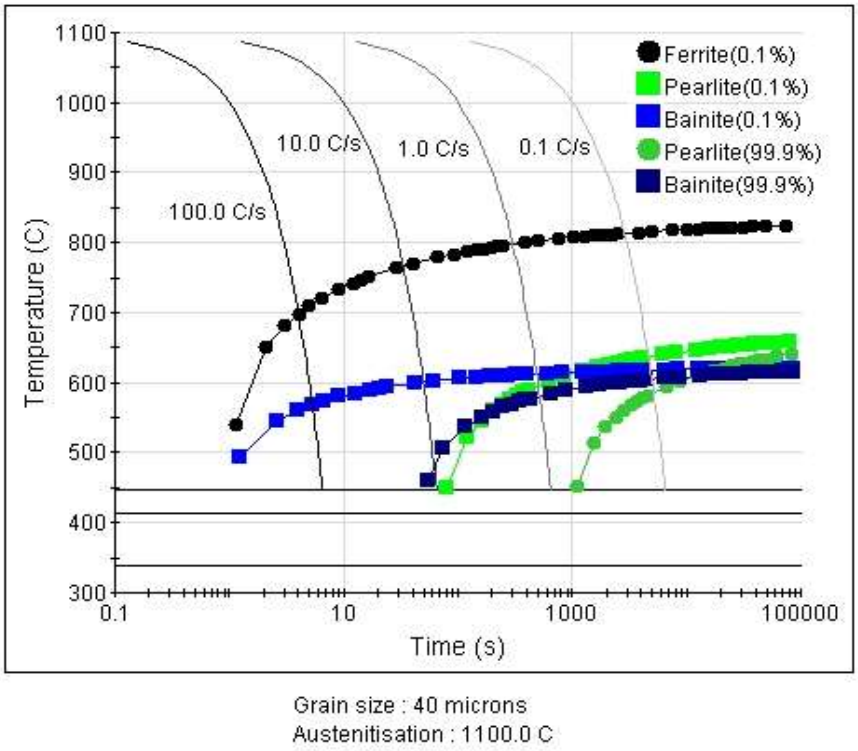

Figure 2.3: Continuous Cooling Transformation (CCT) diagram of the plain C-Mn steel

2.3 Mathematical Modelling

In practical engineering, solid phase transformation is found widely in the steel industries in order to obtain desirable mechanical as well as metallurgical properties of the material through hot rolling, and cooling such as quenching, annealing, martempering, etc. (Mielke and Theil, [89]). Since experiments are unable to provide real time evolution of the phases during cooling of the materials; now-a-days, the researchers are mostly concentrated on the numerical modelling of the process, which is the major concerned of the present work. During heating and cooling, a real time prediction of the phase transformation kinetics of the austenite is possible considering a suitable mathematical model along with appropriate boundary conditions, and suitable consideration of the material properties (Denis *et al.* [90]). In the literature, report on such modelling is very rare. In this context, a systematic mathematical modelling is required to determine the transformation of austenite phase to ferrite, bainite, pearlite, and martensite; along with their transformation time, and the fraction of the transformed phases (Wożeńska *et al.* [91]; Esfahani *et al.* [92]).

The phase transformation mainly depends on heat transfer within the materials during its cooling. Accordingly, a two dimensional (2-D) unsteady state of heat conduction equation is considered to represent the heat transfer within the materials, which is represented as

$$\rho c \frac{\partial T}{\partial t} = \frac{\partial}{\partial x}\left(k \frac{\partial T}{\partial x}\right) + \frac{\partial}{\partial y}\left(k \frac{\partial T}{\partial y}\right) + \rho \frac{dX}{dt} \tag{2.1}$$

where, the last term of the Eq^{n}. 2.1 (volumetric source term) represents evolution of heat during transformation of a phase.

2.3.1 Boundary Conditions

Referring to the Fig. 2.1(b), and in order to understand the phase transformation of plain C-Mn steel, the specimen of the material is heated in the furnace under a controlled heating and cooling conditions as per the Fig. 2.2, where the variation of furnace temperature with time is presented. The process involves heating of the material from ambient temperature (T_{amb}) for a period of $t_{heating}$ to reach a desired temperature or holding temperature ($T_{holding}$). The material is then hold for a period of $t_{holding}$ at this holding temperature ($T_{holding}$) in order to obtain a uniform temperature or austenite phase within the material. After obtaining uniform temperature or phase within the material, it is cooled to the ambient temperature (T_{amb}) at a desired cooling rate (CR) in order to obtain the desired transformed phases within the material.

Accordingly, a function of the furnace temperature with time is considered as T(t). Based on the heating and cooling conditions of the specimen, following appropriate boundary are assumed in order to solve the governing equations.

Top, Left and Right Surfaces:

If, $t \leq t_{heating}$ $\quad T(t) = (T_{holding} - T_{amb}/t_{heating}) \times t + T_{amb}$ (2.2.1)

If, $t_{heating} < t \leq t_{holding} + t_{heating}$ $\quad T(t) = T_{holding}$ (2.2.2)

If, $t > t_{holding} + t_{heating}$ $\quad T(t) = T_{holding} - CR \times (t - t_{holding} - t_{heating})$ (2.2.3)

Bottom Surface: Adiabatic Condition

$$\frac{dT}{dy} = 0 \tag{2.2.4}$$

2.4 Modelling of Phase Transformation

There are several complexities in developing a model for phase transformation in steels, lead to a challenge in implementing and finding numerical solutions (Bzowski *et al.* [93]). It is very crucial to obtain desirable material phases and optimizing the mechanical as well as metallurgical properties. This refers to a suitable modelling of the phase transformation in the solid state. Hence, in order to study transformation of austenite to ferrite, bainite, pearlite, and martensite in steel; development of a phase transformation model is very essential to provide insight of the structural evolution (Dykas *et al.* [94]).

2.4.1 Modelling of the Continuous Cooling Transformation (CCT) Diagram and Identification of the Phases

The Continuous Cooling Transformation (CCT) Diagram presents the beginning and ending of transformation for a phase as a function of time during continuous or isothermal cooling. Based on the extracted data using the JMatPro software for plain C-Mn steel, a polynomial or fitting curve is considered or modelled for beginning as well as ending of transformation of each phase of the transformation. All the modelled equations with respect to start and end of transformation for all the phases are presented in equations (2.3.1-2.3.38). The modelled equations to represent the beginning and ending of transformation for all phases are shown in Fig. 2.4. A good agreement is found for all the phases. Hence, the modelled equations are extended for evolution of the phases during cooling.

2.4.1.1 Equations of the fitting curves for ferrite:

The equations are modelled from the data of CCT diagram extracted using JMatPro for the plain C-Mn steel. 0.1% phase transformation represents the beginning and 99.9% phase transformation represents the ending of the phase transformation.

The equations for the beginning of ferrite phase transformation are:

$$T_{fu} = 533.92, when\ CR \geq 495.89\ (℃/s) \quad (2.3.1)$$

$$T_{fu} = -0.4164CR + 740.41, when\ 99.159 \leq CR < 495.89\ (℃/s) \quad (2.3.2)$$

$$T_{fu} = 0.0047CR^2 - 1.2570CR + 777.56, when\ 11.776 \leq CR < 99.159\ (℃/s) \quad (2.3.3)$$

$$T_{fu} = 0.209CR^2 - 5.69CR + 801.43, when\ 1.219 \leq CR < 11.776\ (℃/s) \quad (2.3.4)$$

$$T_{fu} = -7.13\ln(CR) + 795.42, when\ 0.113 \leq CR < 1.219\ (℃/s) \quad (2.3.5)$$

$$T_{fu} = -4.016\ln(CR) + 798.37, when\ 0.014 \leq CR < 0.113\ (℃/s) \quad (2.3.6)$$

$$T_{fu} = 16145CR^2 - 623.36CR + 811.38, when\ CR < 0.014\ (℃/s) \quad (2.3.7)$$

The equation for the ending of ferrite phase transformation is:

$$T_{fl} = 450 \quad (2.3.8)$$

2.4.1.2 Equations of the fitting curves for bainite:

The equations are modelled from the data of CCT diagram extracted using JMatPro for the plain C-Mn steel. 0.1% phase transformation represents the beginning and 99.9% phase transformation represents the ending of the phase transformation.

The equations for the beginning of bainite phase transformation are:

$$T_{bu} = 497.417, when\ CR \geq 496.72\ (℃/s) \quad (2.3.9)$$

$$T_{bu} = 0.00007CR^2 - 0.2275CR + 593.15, when\ 99.252 \leq CR < 496.72\ (℃/s) \quad (2.3.10)$$

$$T_{bu} = 0.002CR^2 - 0.5512CR + 606.26, when\ 11.774 \leq CR < 99.525\ (℃/s) \quad (2.3.11)$$

$$T_{bu} = 0.064CR^2 - 2.047CR + 615.27, when\ 4.815 \leq CR < 11.774\ (℃/s) \quad (2.3.12)$$

$$T_{bu} = 0.7118CR + 603.47, when\ 3.410 \leq CR < 4.815\ (℃/s) \quad (2.3.13)$$

$$T_{bu} = -0.423CR^2 - 0.0129CR + 610.86, when\ 2.140 \leq CR < 3.410\ (℃/s) \quad (2.3.14)$$

$$T_{bu} = 5.605CR^2 - 22.307CR + 630.96, when\ 1.367 \leq CR < 2.140\ (℃/s) \quad (2.3.15)$$

$$T_{bu} = 3.7418CR^2 - 9.7938CR + 617.34, when\ 0.286 \leq CR < 1.367\ (℃/s) \quad (2.3.16)$$

$$T_{bu} = 121.64CR^2 - 62.69CR + 622.82, when\ 0.162 \leq CR < 0.286\ (℃/s) \quad (2.3.17)$$

$$T_{bu} = -233.55CR^2 + 44.05CR + 614.85, when\ 0.075 \leq CR < 0.162\ (℃/s) \quad (2.3.18)$$

$$T_{bu} = -1001.4CR^2 + 79.021CR + 616.55, when\ 0.022 \leq CR < 0.075\ (℃/s) \quad (2.3.19)$$

$$T_{bu} = -41355CR^2 + 1439.8CR + 606.15, when\ 0.016 \leq CR < 0.022\ (℃/s) \quad (2.3.20)$$

$$T_{bu} = 618.6075, when\ CR < 0.016\ (℃/s) \quad (2.3.21)$$

The equation for the ending of bainite phase transformation is:

$$T_{bl} = 464.53, when\ CR > 11.774\ (℃/s) \quad (2.3.22)$$

$$T_{bl} = -0.0385CR^2 - 10.237CR + 590.4, when\ 1.219 < CR \leq 11.774\ (℃/s) \quad (2.3.23)$$

$$T_{bl} = 7.727CR^2 - 33.058CR + 606.68, when\ 0.189 < CR \leq 1.219\ (℃/s) \quad (2.3.24)$$

$$T_{bl} = -788.94CR^2 + 201.18CR + 590.86, when\ 0.126 < CR \leq 0.189\ (℃/s) \quad (2.3.25)$$

$$T_{bl} = -295.37CR^2 - 19.208CR + 610.79, when\ 0.056 < CR \leq 0.126\ (℃/s) \quad (2.3.26)$$

$$T_{bl} = -4.414\ln(CR) + 603.26, when\ 0.018 \leq CR < 0.056\ (℃/s) \quad (2.3.27)$$

$$T_{bl} = -159.86CR + 613.84, when\ 0.012 < CR \leq 0.018\ (℃/s) \quad (2.3.28)$$

$$T_{bl} = -285.68CR + 615.35, when\ 0.008 < CR \leq 0.012\ (℃/s) \quad (2.3.29)$$

$$T_{bl} = 158171CR^2 - 2607.5CR + 623.8, when\ 0.0056 < CR \leq 0.008\ (℃/s) \quad (2.3.30)$$

$$T_{bl} = 614.152, when\ CR \leq 0.0056\ (℃/s) \quad (2.3.31)$$

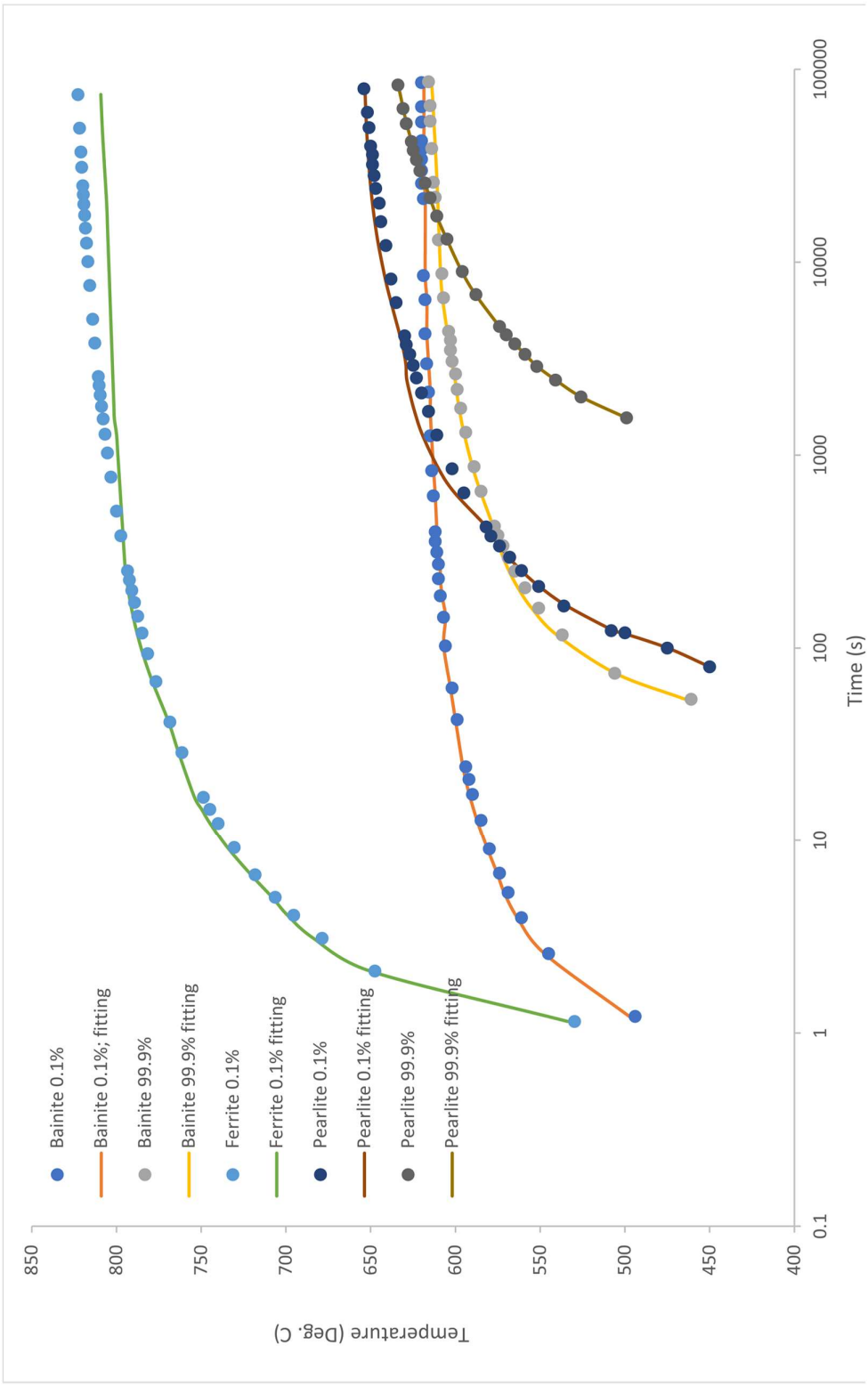

Figure 2.4: Presentation of the fitting curves w.r.t the raw data, indicates beginning (0.1%) and ending (99.9%) of transformation

2.4.1.3 Equations of the fitting curves for pearlite:

The equations are modelled from the data of CCT diagram extracted using JMatPro for the plain C-Mn steel. 0.1% phase transformation represents the beginning and 99.9% phase transformation represents the ending of the phase transformation.

The equations for the beginning of pearlite phase transformation are:

$$T_{pu} = 450.198, when\ CR \geq 8.125\ (℃/s) \tag{2.3.32}$$

$$T_{pu} = 2.7665CR^2 - 52.862CR + 697.07, when\ 4.815 \leq CR < 8.125\ (℃/s) \tag{2.3.33}$$

$$T_{pu} = 0.522CR^2 - 24.00CR + 610.13, when\ 1.219 \leq CR < 4.815\ (℃/s) \tag{2.3.34}$$

$$T_{pu} = 2.9136CR^2 - 50.00CR + 638.27, when\ 0.1898 \leq CR < 1.219\ (℃/s) \tag{2.3.35}$$

$$T_{pu} = 774.55CR^2 - 284.55CR + 654.99, when\ CR < 0.1898\ (℃/s) \tag{2.3.36}$$

The equations for the ending of pearlite phase transformation are:

$$T_{pl} = 450, when\ CR > 0.849(℃/s) \tag{2.3.37}$$

$$T_{pl} = 147.63(CR + 0.635)^2 - 572.87(CR + 0.635) + 975.07, when\ CR < 0.849\ (℃/s) \tag{2.3.38}$$

2.4.2 Cooling Rate Calculation

The cooling rate plays an important role in transformation of the phases in solid state. In the present model as discussed in the section 2.4.1, determination of cooling rate at each point of the computational domain is necessary to identify the phase to be transformed during cooling. Accordingly, a generalised method (as shown in Eq^{n}. 2.4.2) is considered to calculate the cooling rate within the domain of interest. The cooling is considered while the temperature decreases from the temperature of $T_{holding}$. At any instant of temperature (T), respective duration of cooling is calculated by the Eq^{n}. 2.4.1, represented by cooling time (CT). Hence, the total temperature drop is divided by the CT to calculate cooling rate at that instant of time within the domain.

$$CT = t - (t_{heating} + t_{holding}) \tag{2.4.1}$$

$$CR = (T_{holding} - T)/(CT) \tag{2.4.2}$$

2.4.3 Calculation of Transformed Phases

A study on solid phase transformation is needed to obtain desirable mechanical properties of the products. In case of steel, the austenite phase is transformed into ferrite, bainite, pearlite, and martensite or any suitable combination based on the temperature and cooling rate conditions. Now, the fraction of any phase in the product determines its properties. Therefore, consideration of a suitable model is needed to analyse and predict respective fractions of transformation.

As available in the literature, the fraction of any transformed phase is determined using the Avrami equation, which is also known as the Johnson-Mehl-Avrami-Kolmogorov (JMAK) formalization (Barman *et al.* [97]). Serajzadeh [95] stated that the Avrami equation plays a crucial role in determining the progress of phase transformation in any of the material system. This equation is originally developed in respect to heat treatment of the materials; however, it is used widely beyond its conventional use, even in the fields of epidemiology and COVID-19 modelling (Shirzad and Viney, [96]).

The Avrami equation is represented by Eq^{n}. 2.5.1 (Barman *et al.* [97], Biswas *et al.* [98]) in order to calculate the transformation of phase fraction.

$$X = 1 - \exp\left(-b_t t^n\right) \tag{2.5.1}$$

where, X is the transformed fraction of a phase, t is the time of transformation, and b_t and n are constants of respective transformed phase. When austenite is transformed into ferrite phase, the respective constants (Serajzadeh [95]) are considered as

$$b_{tf} = 14.2\, exp\left(-\frac{T - 620}{25.1}\right) and\ n = 0.7 \tag{2.5.2}$$

When austenite is transformed into pearlite or bainite phase, the respective constants (Serajzadeh [95]) are considered as

$$b_{tp}\ or\ b_{tb} = 65.3\, exp\left(-\frac{T - 595}{4.2}\right)\ and\ n = 3.8 \tag{2.5.3}$$

In order to present the transformation behaviour of the phases, the different isothermal transformation of the phases with time are presented in Fig. 2.5 (a, b).

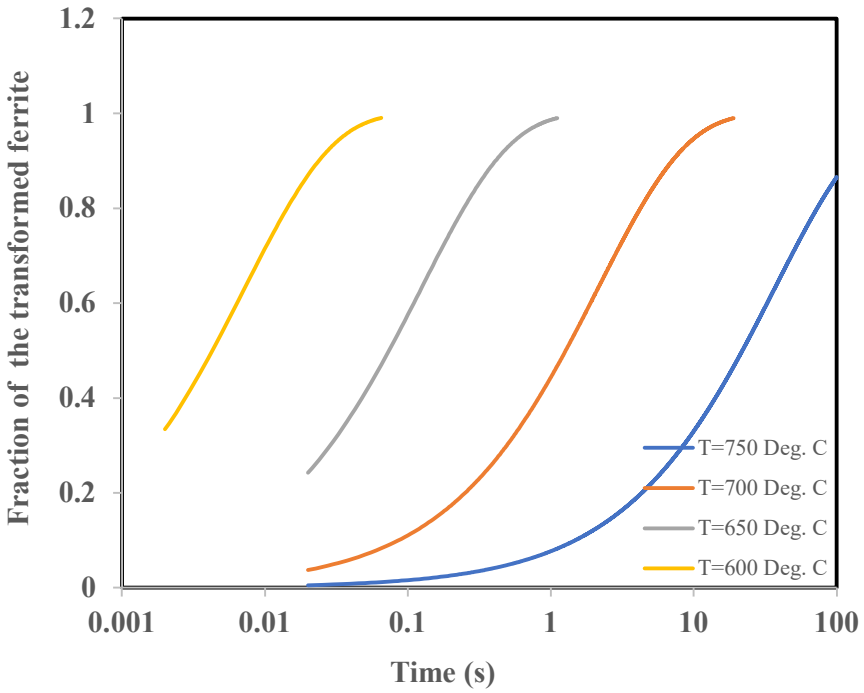

(a)

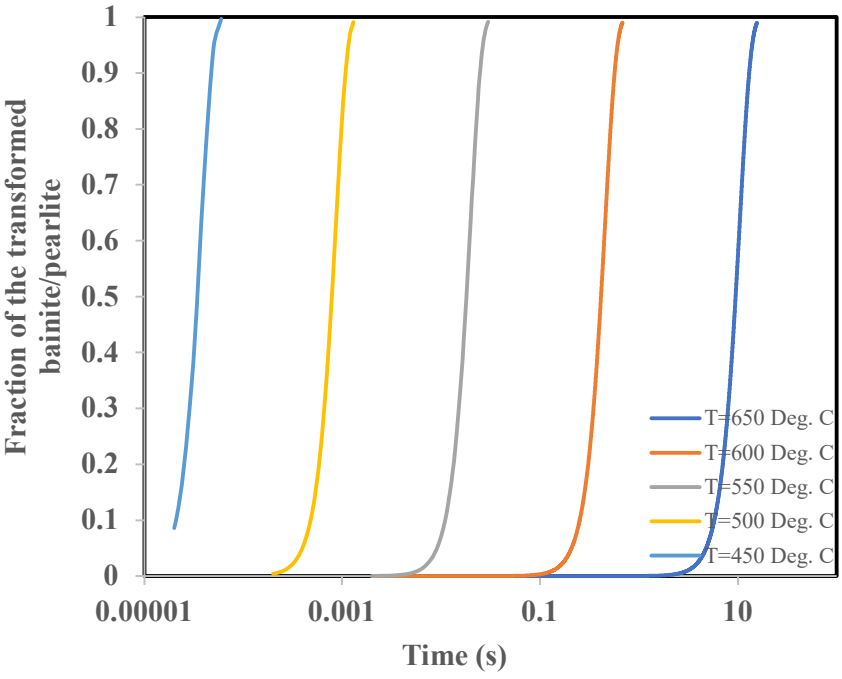

(b)

Figure 2.5: (a) Isothermal transformation of the ferrite phase, and **(b)** Isothermal transformation of the bainite/pearlite phase

2.5 Numerical Modelling

Nowadays, numerical modelling is used widely to solve complex mathematical equations. It is capable of solving various practical applications of engineering, physics, geology, astronomy, aerodynamics, biophysics, nanoscience, etc. Numerical model allows optimal design of the process parameters such as temperature, time, cooling rate, etc. of a process; which is applicable for production of steel or steel sheet also. In case of steel, this process parameters directly correlate with the phase transformation of the steel, determine material properties accordingly (Bzowski *et al.* [99]; Militzer *et al.* [100]; Rezaei *et al.* [101]).The numerical simulation plays a vital role in the field of advancement of steel, a footprint in developing the next generation steel (Chen *et al.* [102]). Respective innovative predictions are helpful in obtaining desirable properties, which thereby empowers the optimization of steel processing, material behaviour, and formation of high-performance steels.

Accordingly, this work considers a suitable numerical modelling of the governing equation and boundary conditions as presented in the section 2.3 and subsequent modelling of the phase transformation. The governing equation is mainly the conservation of energy, leads to consider the finite volume method (FVM) of discretization. The discretization of the equation is presented here (Eq^{n}. 2.6.1-2.6.14) following the methods presented in Patankar [103].

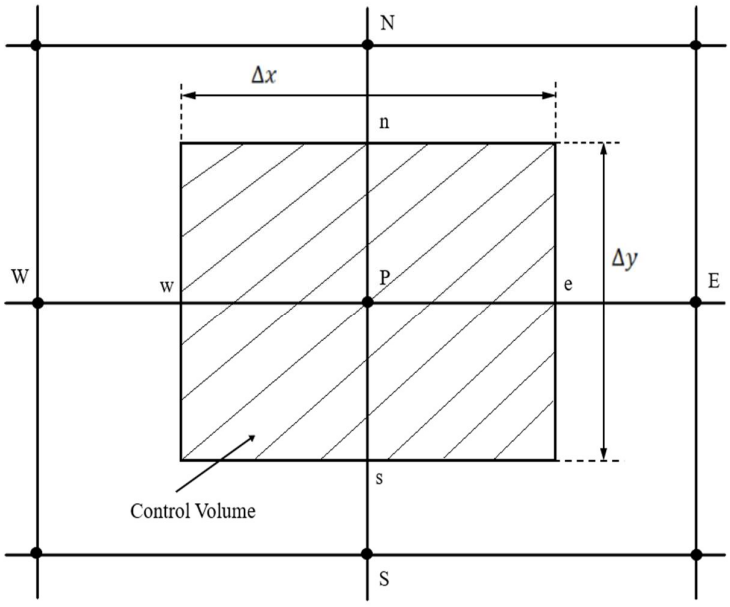

Figure 2.6: A sample control volume of the two-dimensional computational domain

Fig. 2.6 represents a sample control volume of the two-dimensional computational domain (small letters represent faces of the control volume, and capital letters represent the nodes/grids of the discretized domain), the referred governing Eq[n]. 2.1 is simplified as

$$\rho c \frac{\partial T}{\partial t} = \frac{\partial}{\partial x}\left(k \frac{\partial T}{\partial x}\right) + \frac{\partial}{\partial y}\left(k \frac{\partial T}{\partial y}\right) + S \tag{2.6.1}$$

where, S is the volumetric source term represents heat evolution during phase transformation

$$S = \rho \frac{dX}{dt} \tag{2.6.2}$$

The above equation (Eq[n]. 2.6.1) is integrated based on the finite volume method over the control volume as shown in Fig. 2.6.

$$\rho c \int_w^e \int_s^n \int_t^{t+\Delta t} \frac{\partial T}{\partial t} dt dy dx = \int_t^{t+\Delta t} \int_s^n \int_w^e \left[\frac{\partial}{\partial x}\left(k \frac{\partial T}{\partial x}\right) + \frac{\partial}{\partial y}\left(k \frac{\partial T}{\partial y}\right) + S\right] \tag{2.6.3}$$

In case of the transient term, a uniformity of temperature is considered within the control volume. Accordingly,

$$\rho c \int_w^e \int_s^n \int_t^{t+\Delta t} \frac{\partial T}{\partial t} dt dy dx = \rho c \Delta x \Delta y (T_P^1 - T_P^0) \tag{2.6.4}$$

where superscript '1' represents the new value of temperature at the node P, whereas superscript '0' represents old value of the temperature at same node. The diffusion terms at steady-state condition are discretized considering respective face properties and the temperature of adjacent nodes. Therefore, Eqn. 2.6.3 becomes

$$\rho c \Delta x \Delta y (T_P^1 - T_P^0) = \int_t^{t+\Delta t} \left\{ \left[\frac{k_e \Delta y (T_E - T_P)}{(\delta x)_e} - \frac{k_w \Delta y (T_P - T_W)}{(\delta x)_w} \right] + \left[\frac{k_n \Delta x (T_N - T_P)}{(\delta y)_n} - \frac{k_w \Delta y (T_P - T_S)}{(\delta y)_s} \right] + S \Delta x \Delta y \right\} \quad (2.6.5)$$

where, the source term is further represented as $S = S_c + S_p T_p$, in order to separate the constant and variable parts of the source.

The integration of the right hand side of the Eq^{n}. 2.6.5 is considered as follows

$$\int_t^{t+\Delta t} T_P dt = [f T_P^1 - (1-f) T_P^0] \Delta t \quad (2.6.6)$$

where, *f* is the weighting factor ranging between 0 and 1.

The final discretised equation is obtained and rearranged as

$$\rho c \frac{\Delta x \Delta y}{\Delta t} \left(T_p^1 - T_p^0\right) = f \left[\frac{k_e \Delta y (T_E^1 - T_P^1)}{(\delta x)_e} - \frac{k_w \Delta y (T_P^1 - T_W^1)}{(\delta x)_w} \right] + (1-f) \left[\frac{k_e \Delta y (T_E^0 - T_P^0)}{(\delta x)_e} - \frac{k_w \Delta y (T_P^0 - T_W^0)}{(\delta x)_w} \right] + f \left[\frac{k_n \Delta x (T_N^1 - T_P^1)}{(\delta y)_n} - \frac{k_s \Delta x (T_P^1 - T_S^1)}{(\delta y)_s} \right] + (1-f) \left[\frac{k_n \Delta x (T_N^0 - T_P^0)}{(\delta y)_n} - \frac{k_s \Delta x (T_P^0 - T_S^0)}{(\delta y)_s} \right] + S_c \Delta x \Delta y + S_P T_P \Delta x \Delta y \quad (2.6.7)$$

$$\Rightarrow \rho c\frac{\Delta x\Delta y}{\Delta t}\left(T_p^1\right)-\rho c\frac{\Delta x\Delta y}{\Delta t}\left(T_p^0\right)$$
$$=f\left(\frac{k_e\Delta y}{(\delta x)_e}T_E^1\right)-f\left(\frac{k_e\Delta y}{(\delta x)_e}T_P^1\right)-f\left(\frac{k_w\Delta y}{(\delta x)_w}T_P^1\right)+f\left(\frac{k_w\Delta y}{(\delta x)_w}T_W^1\right)$$
$$+(1-f)\left(\frac{k_e\Delta y}{(\delta x)_e}T_E^0\right)-(1-f)\left(\frac{k_e\Delta y}{(\delta x)_e}T_P^0\right)-(1-f)\left(\frac{k_w\Delta y}{(\delta x)_w}T_P^0\right)$$
$$+(1-f)\left(\frac{k_w\Delta y}{(\delta x)_w}T_W^0\right)+f\left(\frac{k_n\Delta x}{(\delta y)_n}T_N^1\right)-f\left(\frac{k_n\Delta x}{(\delta y)_n}T_P^1\right)-f\left(\frac{k_s\Delta x}{(\delta y)_s}T_P^1\right)$$
$$+f\left(\frac{k_s\Delta x}{(\delta y)_s}T_S^1\right)+(1-f)\left(\frac{k_n\Delta x}{(\delta y)_n}T_N^0\right)-(1-f)\left(\frac{k_n\Delta x}{(\delta y)_n}T_P^0\right)$$
$$-(1-f)\left(\frac{k_s\Delta x}{(\delta y)_s}T_P^0\right)+(1-f)\left(\frac{k_s\Delta x}{(\delta y)_s}T_S^0\right)+S_c\Delta x\Delta y+S_PT_P\Delta x\Delta y$$

(2.6.8)

$$\rho c\frac{\Delta x\Delta y}{\Delta t}\left(T_p^1\right)+f\left(\frac{k_e\Delta y}{(\delta x)_e}T_P^1\right)+f\left(\frac{k_w\Delta y}{(\delta x)_w}T_P^1\right)+f\left(\frac{k_n\Delta x}{(\delta y)_n}T_P^1\right)+f\left(\frac{k_s\Delta x}{(\delta y)_s}T_P^1\right)$$
$$=\rho c\frac{\Delta x\Delta y}{\Delta t}\left(T_p^0\right)+f\left(\frac{k_e\Delta y}{(\delta x)_e}T_E^1\right)+f\left(\frac{k_w\Delta y}{(\delta x)_w}T_W^1\right)+f\left(\frac{k_n\Delta x}{(\delta y)_n}T_N^1\right)$$
$$+f\left(\frac{k_s\Delta x}{(\delta y)_s}T_S^1\right)+(1-f)\left(\frac{k_e\Delta y}{(\delta x)_e}T_E^0\right)-(1-f)\left(\frac{k_e\Delta y}{(\delta x)_e}T_P^0\right)$$
$$-(1-f)\left(\frac{k_w\Delta y}{(\delta x)_w}T_P^0\right)+(1-f)\left(\frac{k_w\Delta y}{(\delta x)_w}T_W^0\right)+(1-f)\left(\frac{k_n\Delta x}{(\delta y)_n}T_N^0\right)$$
$$-(1-f)\left(\frac{k_n\Delta x}{(\delta y)_n}T_P^0\right)-(1-f)\left(\frac{k_s\Delta x}{(\delta y)_s}T_P^0\right)+(1-f)\left(\frac{k_s\Delta x}{(\delta y)_s}T_S^0\right)$$
$$+S_c\Delta x\Delta y+S_PT_P\Delta x\Delta y$$

(2.6.9)

To simplify the equation, following terms are considered

$$a_E=\frac{k_e\Delta y}{(\delta x)_e},a_W=\frac{k_w\Delta y}{(\delta x)_w},a_N=\frac{k_n\Delta x}{(\delta y)_n},a_S=\frac{k_s\Delta x}{(\delta y)_s},a_P^0=\rho c\frac{\Delta x\Delta y}{\Delta t}$$

Instead of using superscript '1', $T_P, T_E, T_W, T_N, and\ T_S$ represent the new values of T at time $t+\Delta t$. Therefore, the Eq^{n}. (2.6.9) becomes

$$a_P^0 T_P + f a_E T_P + f a_W T_P + f a_N T_P + f a_S T_P - S_P T_P \Delta x \Delta y$$
$$= a_P^0 T_P^0 + + f a_E T_E + f a_W T_W + f a_N T_N + f a_S T_S + (1-f) a_E T_E^0$$
$$- (1-f) a_E T_P^0 - (1-f) a_W T_P^0 + (1-f) a_W T_W^0 + (1-f) a_N T_N^0$$
$$- (1-f) a_N T_P^0 - (1-f) a_S T_P^0 + (1-f) a_S T_S^0 + S_c \Delta x \Delta y$$

(2.6.10)

Let,

$$a_P = a_P^0 + f a_E + f a_W + f a_N + f a_S - S_P \Delta x \Delta y$$

(2.6.11)

Then the equation (Eq^n. 2.6.10) is finally rearranged as

$$a_P T_P = a_E [f T_E + (1-f) T_E^0] + a_W [f T_W + (1-f) T_W^0] + a_N [f T_N + (1-f) T_N^0]$$
$$+ a_S [f T_S + (1-f) T_S^0]$$
$$+ [a_P^0 - (1-f) a_E - (1-f) a_W - (1-f) a_N - (1-f) a_S] T_P^0$$
$$+ S_c \Delta x \Delta y$$

(2.6.12)

which is the final discretized equation of the governing equation (Eq^n. 2.1).

2.5.1 Consideration of Crank-Nicolson Scheme

There are usually three kinds of scheme to solve the discretized equation where the weighting factor *f* varies as 0 in case of explicit scheme, 0.5 in case of crank nicolson scheme, and 1 in case of implicit scheme. Consideration of a variable (its old and new values) under the different schemes is presented in Fig. 2.7.

The present work considers the Crank-Nicolson scheme, where the weighting factor is considered as 0.5. Accordingly, the equation (Eq^n. 2.6.12) is modified as

$$a_P T_P = a_E \left(\frac{1}{2} T_E + \frac{1}{2} T_E^0\right) + a_W \left(\frac{1}{2} T_W + \frac{1}{2} T_W^0\right) + a_N \left(\frac{1}{2} T_N + \frac{1}{2} T_N^0\right)$$
$$+ a_S \left(\frac{1}{2} T_S + \frac{1}{2} T_S^0\right) + \left[a_P^0 - \frac{1}{2} a_E - \frac{1}{2} a_W - \frac{1}{2} a_N - \frac{1}{2} a_S\right] T_P^0 + S_c \Delta x \Delta y$$

(2.6.13)

$$\Rightarrow a_P T_P = \frac{a_E}{2}(T_E + T_E^0) + \frac{a_W}{2}(T_W + T_W^0) + \frac{a_N}{2}(T_N + T_N^0) + \frac{a_S}{2}(T_S + T_S^0) + \left[a_P^0 - \frac{1}{2}a_E - \frac{1}{2}a_W - \frac{1}{2}a_N - \frac{1}{2}a_S\right] T_P^0 + S_c \Delta x \Delta y$$

(2.6.14)

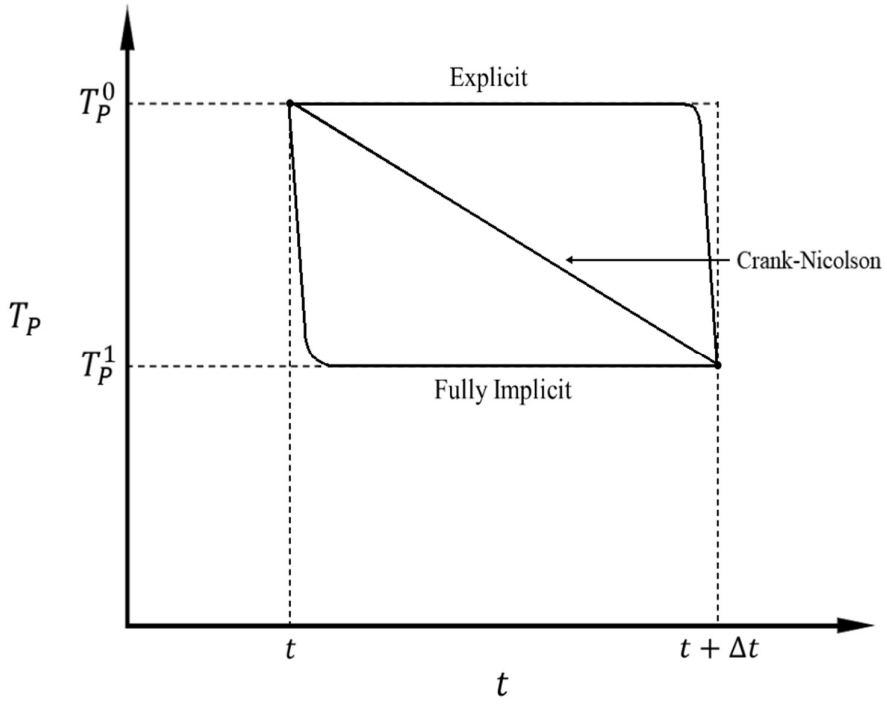

Figure 2.7: Variation of temperature with time under different schemes

2.5.2 Convergence Criteria

Eq[n]. 2.6.14 provides simultaneous linear equations for the considered numerical domain of solution. These simultaneous equations along with the appropriate boundary conditions are solve based on the tri-diagonal matrix algorithm (TDMA). While solving the simultaneous equations a convergence criterion as presented in the Eq[n]. 2.7 is considered in the present work. The convergence criteria considering the present work is

$$\left|\frac{(\phi - \phi_{old}}{\phi_{max}}\right| < 10^{-4}$$

(2.7)

where,

ϕ represents the variable at a grid point of current iteration,

ϕ_{old} represents value of the variable at its preceding iteration,

ϕ_{max} is the maximum value of the variable within domain of current iteration.

2.6 Closure

The present chapter considered a physical problem relating to the objective of the thesis, subsequent modelling of the problem with appropriate boundary conditions, modelling of the solid phase transformation of plain C-Mn steel. The respective governing equation is discretized based on the finite volume method (FVM) using Crank Nicolson scheme, and then TDMA is considered to solve the linear simultaneous equations with a suitable convergence criterion.

References

[82]. Y. Tian, M. Zhao, W. Liu, J. Zhang, M. Zhang, H. Li, D. Yin, and A. Atrens, Comparison on tensile characteristics of plain C-Mn steel with ultrafine grained ferrite/cementite microstructure and coarse grained ferrite/pearlite microstructure, *Materials*, Vol. 14, 2021, 2309

[83]. C. G. Jeong, T. T. T. Trang, Y. Woo, E. Y. Yoon, Y. Lee, and Y. U. Heo, Effect of cooling rate on the final microstructure and tensile property in an Fe-Mn-Si-C based multiphase TRIP steel, *Materials Science & Engineering A*, Vol. 887, 2023, 145696

[84]. A. Karmakar, P. Sahu, S. Neogy, D. Chakrabarti, R. Mitra, S. Mukherjee, and S. Kundu, Effect of Cooling Rate and Chemical Composition on Microstructure and Properties of Naturally Cooled Vanadium-Microalloyed Steels, *Metallurgical and Materials Transactions A*, Vol. 48, 2017, pp. 1581-1595

[85]. J. Trzaska, A. Jagiełło, and L. A. Dobrzański, The Calculation of CCT diagrams for engineering steels, *Archives of Materials Science and Engineering*, Vol. 39 (1), 2009, pp. 13-20

[86]. H. Martin, P. A. Yirenkyi, A. Pohjonen, N. K. Frempong, J. Komi, and M. Somani, Statistical modelling for prediction of CCT diagrams of steel involving interaction of alloying elements, *Metallurgical and Materials Transactions B*, Vol. 52B, 2021, pp. 223-235

[87]. K. Halmešová, R. Procházka, M. Koukolíková, J. Džugan, P. Konopík, and T. Bucki, Extended continuous cooling transformation (CCT) diagrams determination for additive manufacturing deposited steels, *Materials*, Vol. 15, 2022, 3076

[88]. I. Schindler, R. Kawulok, P. Opěla, P. Kawulok, S. Rusz, J. Sojka, M. Sauer, H. Navrátil, and L. Pindor, Effects of austenitization temperature and pre-deformation on CCT diagrams of 23MnNiCrMo5-3 steel, *Materials*, Vol. 13, 2020, 5116

[89]. A. Mielke, and F. Theil, A mathematical model for rate-independent phase transformations with hysteresis, *Proceedings of the workshop on Models of Continuum Mechanics in Analysis and Engineering*, 1999, pp. 117-129

[90]. S. Denis, D. Farias, and A. Simon, Mathematical Model Coupling Phase Transformations and Temperature Evolutions in Steels, *ISIJ International*, Vol. 32 (3), 1992, pp. 316-325

[91]. I. O. Wożeńska, H. Adrian, B. Mrzygłód, and M. Głowacki, Mathematical model of bainitic transformation in austempered ductile iron, *Archives of Foundry Engineering*, Vol. 17 (4), 2017, pp. 200-206

[92]. A. K. Esfahani, M. Babaei, and S. S. Foroushani, A numerical model coupling phase transformation to predict microstructure evolution and residual stress quenching of 1045 steel, *Mathematics and Computers in Simulation*, Vol. 179, 2021, pp. 1-22

[93]. K. Bzowski, Ł. Rauch, M. Pietrzyk, M. Kwiecień, and K. Muszka, Numerical Modelling of Phase Transformations in dual-phase steels using level set and SSRVE approaches, *Materials*, Vol. 14, 2021, 5363

[94]. J. Dykas, L. Samek, A. Grajcar, and A. Kozłowska, Modelling of phase diagrams and continuous cooling transformations diagrams of medium manganese steel, *Symmetry*, Vol. 15, 2023, 381

[95]. S. Serajzadeh, Modelling of temperature history and phase transformations during cooling of steel, *Journal of Materials Processing Technology*, Vol. 146, 2004, pp. 311-317

[96]. K. Shirzad, and C. Viney, A critical review on applications of the Avrami equation beyond materials science, *Journal of the Royal Society Interface*, Vol. 20 (203), 2023, 20230242

[97]. S. Barman, N. Barman, A. Mukhopadhyay, and S. Sen, A Numerical Study on the Phase Transformation behaviour during Cooling of a Moving Plate, *Proceedings of the 21st National & 10th ISHMT-ASME Heat and Mass Transfer Conference*, *IIT Madras, India*, 2011

[98]. S. K. Biswas, S. J. Chen, and A. Satyanarayana, Optimal temperature tracking for accelerated cooling processes in hot rolling steel, *Dynamics and Control*, Vol. 7, 1997, pp. 327-340

[99]. K. Bzowski, Ł. Rauch, M. Pietrzyk, M. Kwiecień, and K. Muszka, Numerical Modelling of Phase Transformations in dual-phase steels using level set and SSRVE approaches, *Materials*, Vol. 14, 2021, 5363

[100]. M. Militzer, J. J. Hoyt, N. Provatas, J. Rottler, C. W. Sinclair, and H. S. Zurob, Multiscale Modelling of Phase Transformations in Steels, *The Minerals, Metals and Materials Society*, Vol. 66 (5), 2014, pp. 740-746

[101]. J. Rezaei, M. H. Parsa, and H. Mirzadeh, Phase transformation kinetics of high-carbon steel during continuous heating, *Journal of Materials Research and Technology*, Vol. 27, 2023, pp. 2524-2537

[102]. S. F. Chen, K. Bandyopadhyay, S. Basak, B. Hwang, J. H. Shim, J. Lee, and M. G. Lee, Predictive integrated numerical approach for modelling spatio-temporal microstructure evolution and grain size dependent phase transformations in steel, *International Journal of Plasticity*, Vol. 139, 2021, 102952

[103]. S. V. Patankar, Numerical Heat Transfer and Fluid Flow, 1st Edition, CRC Press, New York, 1980

CHAPTER – III

Results and Discussion

3.1 Introduction

This work considers a numerical study on solid phase transformation of a plain C-Mn steel under different cooling rate conditions. Accordingly, the work considers a suitable problem referring to the furnace of heating, holding, and cooling of the plain C-Mn steel. Then a suitable mathematical model to represent the heating and cooling process, is considered using the energy equation along with a volumetric source term representing evolution of heat due to phase transformation. The major challenge in this work is the identification of phases to be transformed during cooling of the steel. Thus, the continuous cooling transformation (CCT) diagram of the plain C-Mn steel is modelled based on the cooling rate and transformation temperature those identify the phase/s of transformation.

The governing equation is discretized based on the finite volume method (FVM) using the Crank-Nicolson scheme. Subsequently, a code is developed on the FORTRAN platform in order to predict the temperature history of the process, cooling rate, fraction of transformed phases, etc. The developed code is validated with a cited literature; shows a good agreement and, hence, includes a parametric study.

3.2 Development of a FORTRAN based numerical code

This work is a numerical simulation of solid phase transformation of a material, i.e., a plain C-Mn steel, includes prediction of the temperature, cooling rate and phase distributions, and subsequent prediction of phase transformation time of the respective phases. In this context, a numerical code is developed on the FORTRAN platform to solve the simultaneous equations in association with the necessary boundary conditions using the tri-diagonal matrix algorithm (TDMA). It is worth to mention here that the respective discretization is performed based on the finite volume method (FVM) using the Crank-Nicolson scheme.

The developed code is then tested for the necessary grid independence study. In this context, a set of different uniform grids is considered as 62×42, 82×62, and 92×72 for grid independence study. Under these different grid conditions, the variation of temperature at mid-point of the specimen/ computational domain is presented in the Fig. 3.1. It is found that the variation of temperature at higher grid condition is similar to that of the 62×42 grid condition with more computational time. Thus, in the present work, the 62×42 grid system is considered for final analysis of the physical problem.

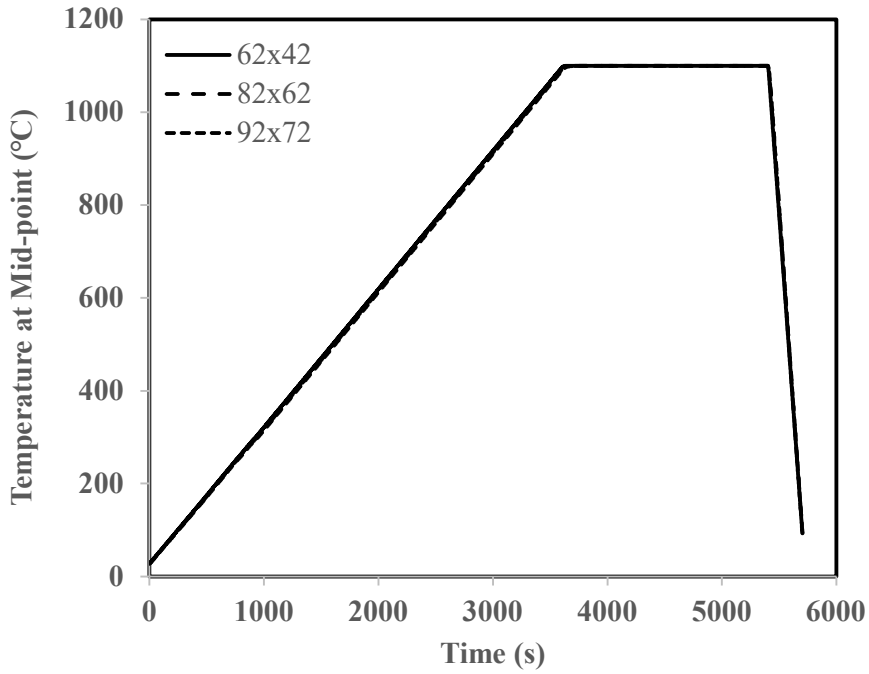

Figure 3.1: Variation of temperature with time at mid-point of the specimen under consideration of different grid systems

3.3 A Case Study with a specimen of plain C-Mn steel

A material of the plain C-Mn steel with the dimensions of 5mm×5mm×5mm as a specimen, is considered for study of related heat transfer and subsequent transformation of the phases under a cooling rate of 3.33 ℃/s. It is considered that the specimen is initially heated at a rate of 0.345 ℃/s from ambient temperature of 28℃ for a time period of 3600s, and then it is holded at a temperature of 1100℃ for a time period of 1800s. After attaining the uniform holding temperature (1100℃), the specimen is cooled continuously at a cooling rate of 3.33 ℃/s to the ambient temperature of 28℃. The respective variation of the temperature representing heating, holding, and cooling is presented as the furnace temperature in the Fig. 3.2.

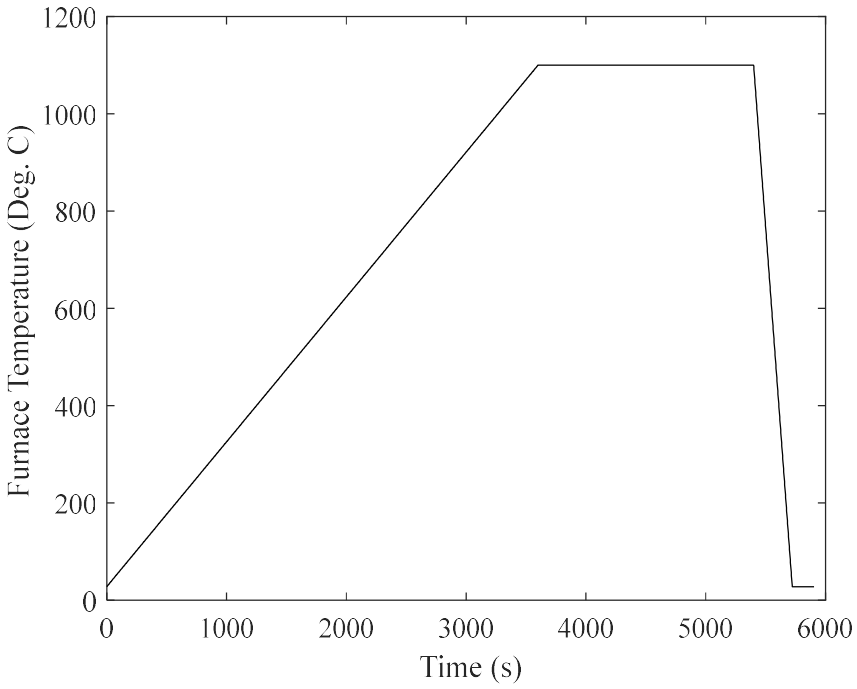

Figure 3.2: Variation of furnace temperature with time

3.3.1 Transformation phenomena and evolution of phases during cooling

During cooling, the material undergoes a phase transformation depending on temperature and cooling rate within the domain of interest. After holding the specimen at 1100℃, the temperature in the entire domain attains 1100℃. Then, a cooling rate of 3.33 ℃/s is set at boundary to cool the specimen, along with the boundary conditions as specified in the Chapter-II, and sub-section 2.3.1. Subsequent, evolution of the temperature distribution within the computational domain is presented in the Fig. 3.3 at different times. The periphery of the specimen cools first rather than bottom centre of the specimen. As time increases, the temperature of the entire domain decreases due to cooling. It is further noted that a temperature difference maximum of about 10℃ attains between the bottom centre and periphery of the specimen.

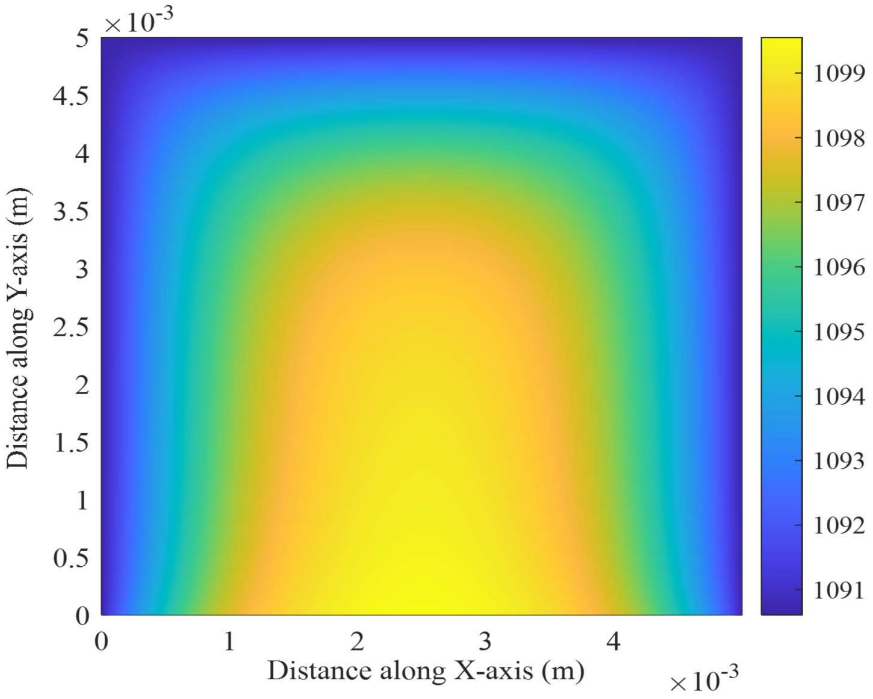

(a)

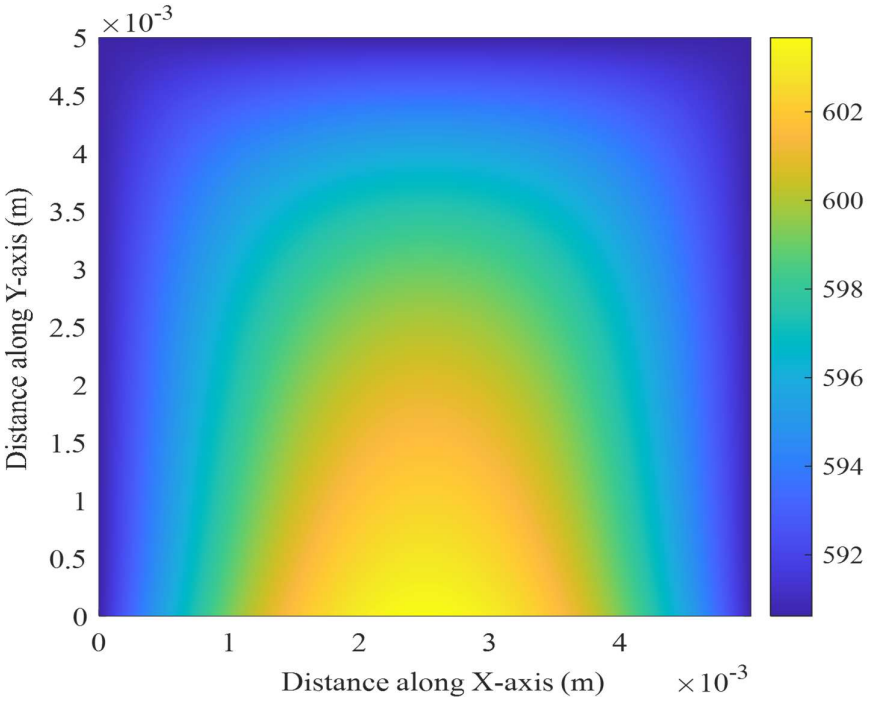

(b)

Figure 3.3: Distribution of temperature at different times: **(a)** t = 5400s, and **(b)** t = 5550s

Based on the time dependent temperature distribution and considering the Eq^{n}. 2.5.2, the distribution of cooling rate with time is predicted and presented in the Fig. 3.4 corresponds to the time of the mentioned temperature distribution of the Fig. 3.3. At beginning of the cooling process, peripheral cooling rate is comparatively higher than that of the bottom centre of the specimen. A cooling rate of about 3.33 ℃/s is obtained at the periphery of the specimen, whereas it has a zero value at bottom centre of the specimen as shown in Fig. 3.4(a). As time increases, effect of the cooling penetrates towards bottom centre of the specimen, and a uniform distribution of cooling is found to a value of about 3.33 ℃/s in the entire domain as shown in Fig. 3.4(b).

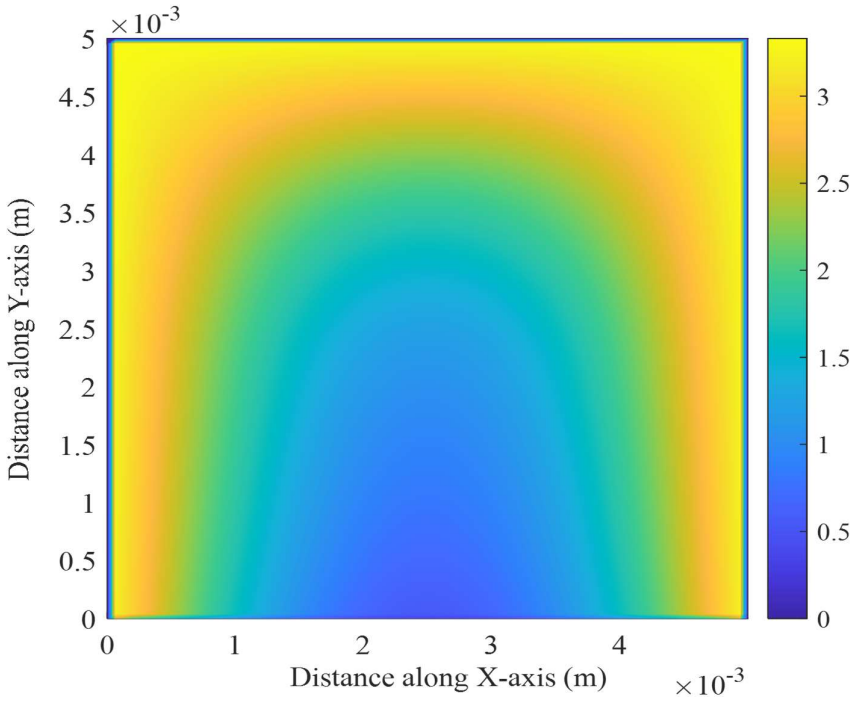

(a)

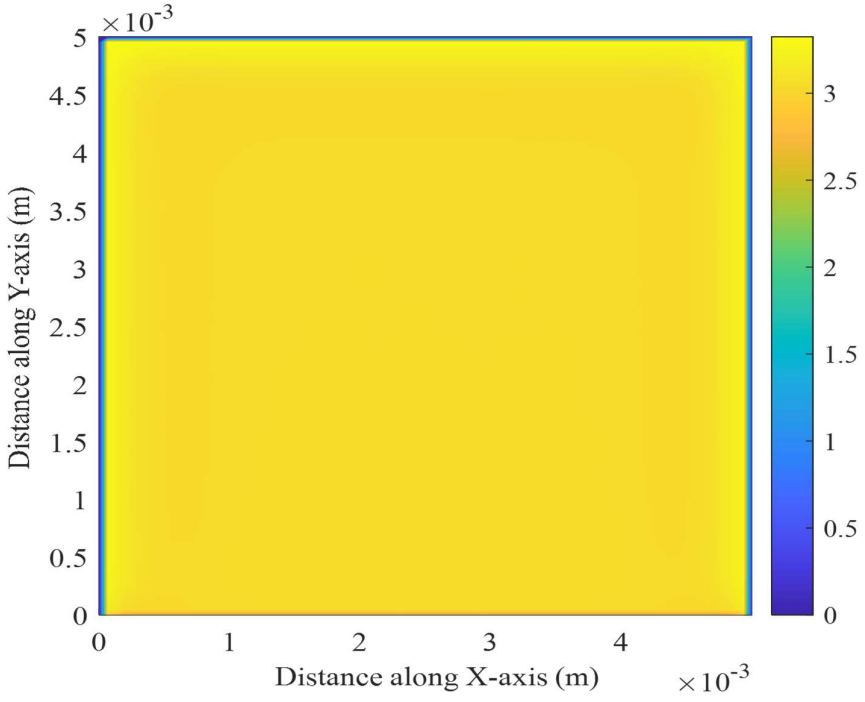

(b)

Figure 3.4: Distribution of cooling rate at different times: **(a)** t = 5400s, and **(b)** t = 5550s

Phase transformation of a material occurs during its cooling. In order to understand insight of the phase transformation of a material, prediction of the temperature and cooling rate distributions within the domain is essential. Based on the temperature and cooling rate distributions presented in the Fig. 3.3 and 3.4, respectively for the mentioned times, and the model considered for the continuous cooling transformation (CCT) diagram presented in the Fig. 2.4 (Chapter-II, sub-section 2.4.1) along with the Eq^{n}. (2.3.1-2.3.38); the transformation of a phase is identified first. After identification of the phases, the transformed fraction of the phases is calculated using the Avrami equation (Eq^{n}.2.5.1). Respective evolution of the phases, i.e., ferrite, bainite, and pearlite with time is presented in the Fig. 3.5. It is found that the transformation of the ferrite phase starts first at about 5494s (i.e., 94s after starting of cooling at 3.33 °C/s) according to the CCT diagram and continue its transformation upto about 5594s.

Hence, the ferrite phase transformation occurs over a time of about 100s, and as a result, a total of 0.79 fraction of the austenite is transformed to ferrite. The bainite phase starts its transformation at about 5548s (i.e., 148s after starting of cooling at 3.33 ℃/s) and continues its transformation upto about 5563s over a period of 15s to the fraction of 0.048 of the austenite. Similar to the bainite, pearlite starts its transformation at about 5561s (i.e., 161s after starting of cooling at 3.33 ℃/s) and continues its transformation upto about 5594s over a period of 33s to the fraction of 0.16 of the austenite. Based on the consequences of above times, different time slots of the phase transformation are presented in the Table.3.1. Initially only the ferrite phase is transformed over a period of 54s, and then the bainite phase is transformed along with the ferrite phase over a period of 13s. It is observed that all the three phases (ferrite, bainite, and pearlite) transformed together over a period of 3s, then ferrite and pearlite combinedly transformed over a period of 31s. It is observed that these transformations follow the modelling of the CCT diagram.

Table. 3.1. Transformation time of the phases

Phases	***Span of the transformation time after cooling starts (cooling starts at 5400s)***			
Ferrite	94s-147s	148s-160s	161s-163s	164s -194s
Bainite		148s-160s	161s-163s	
Pearlite			161s-163s	164s -194s

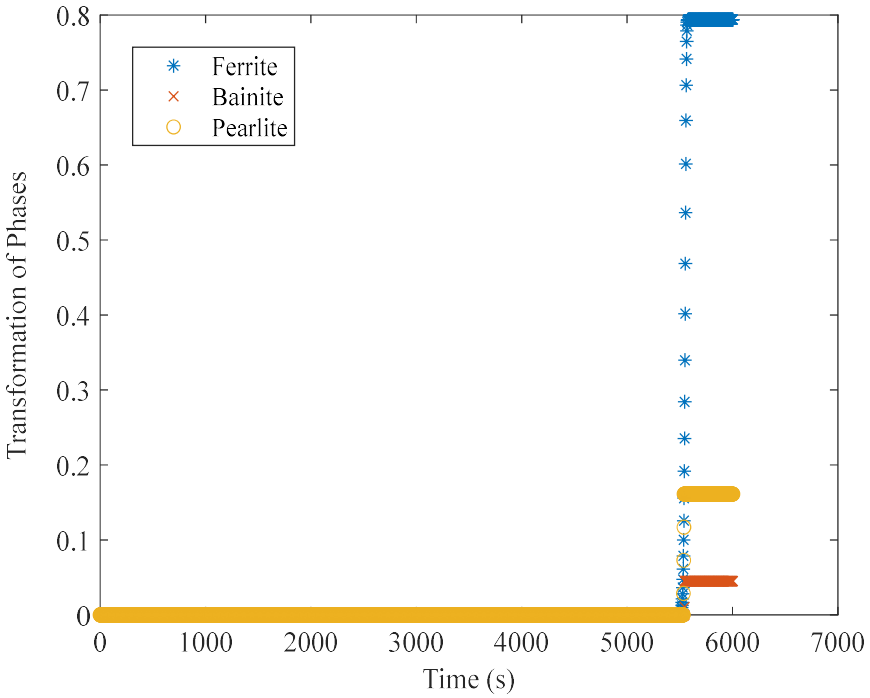

Figure 3.5: Evolution of the phases (ferrite, bainite, and pearlite) with time

It is found that the ferrite phase transforms over a period of about 100s, whereas the bainite and pearlite phases transform over a period of 15s and 33s, respectively. Since, ferrite transformation takes place over a longer period of time, its evolution with time is presented in the Fig. 3.6 (a), (b), (c), and (d). After heating the specimen to the temperature of 1100°C and holding it at that temperature upto the period of 5400s; the specimen starts cooling. The phase transformation of the ferrite phase starts at about 94s after starting of cooling. After about 97s of the cooling, a fractional amount of transformed ferrite is obtained about 1.8×10^{-4} near the periphery of the specimen, as presented in the Fig. 3.6 (a). As observed, the austenite transformation to ferrite takes place mostly near to the periphery of the specimen following the cooling rate distribution, as presented in the Fig. 3.4 (a). As transformation time increases, the fraction of transformed ferrite increases from periphery towards bottom centre of the specimen. After 120s of the cooling, the fraction of transformed ferrite is obtained as 0.016 near to the periphery of the specimen as presented in the Fig. 3.6 (b). Similarly, after 150s and 180s of the cooling, the fractions of transformed ferrite are obtained as 0.46 and 0.79, respectively. It is further observed that, as the time of transformation increases, the difference between the peripheral fraction of transformed ferrite to that at bottom centre increases first and then decreases with time as presented in the Table. 3.2. At the initial state of transformation,

peripheral cooling rate is comparatively higher than that at the bottom centre, which results increase in the difference of fraction of transformation at the periphery compared to that at the bottom centre. At later stage of the transformation, cooling penetrates towards the bottom centre of the specimen, which increases transformed fraction near to the bottom centre of the specimen also. Accordingly, the difference between the peripheral fraction of transformed ferrite to that at bottom centre decreases.

Table 3.2: Fractional difference in peripheral and bottom centre transformed ferrite

Time after cooling starts (cooling starts at 5400s)	***Difference between the peripheral and bottom centre fractional transformed ferrite***
97s	0.00018
120s	0.006
150s	0.12
180s	0.00008
194s	0.00

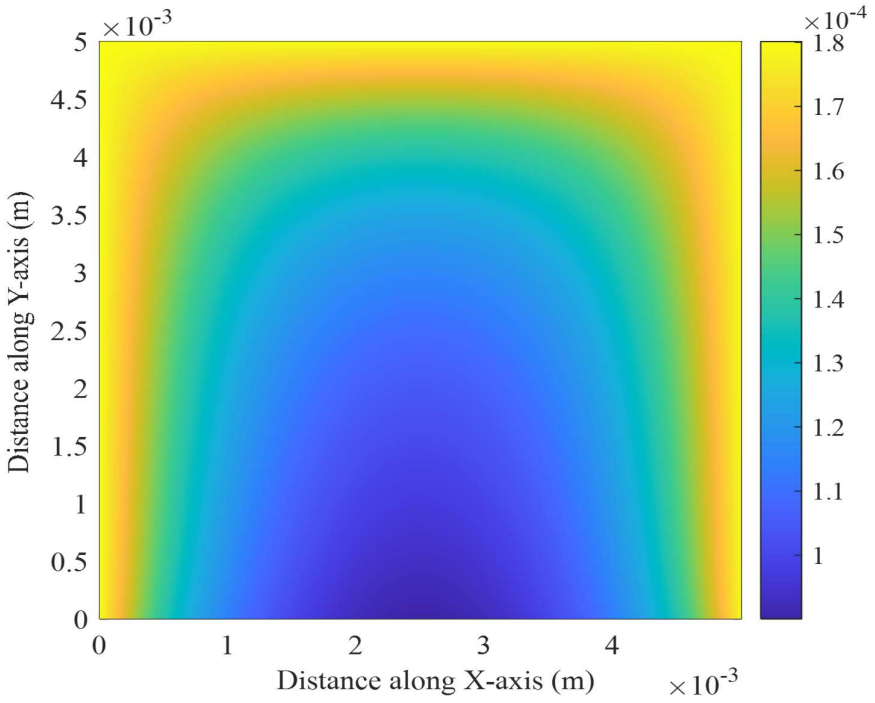
×10-3
5
4.5
4
3.5
3
2.5
2
1.5
1
0.5
0
Distance along Y-axis (m)
0
1
2
3
4
Distance along X-axis (m)
×10-3
×10-4
1.8
1.7
1.6
1.5
1.4
1.3
1.2
1.1
1

(a)

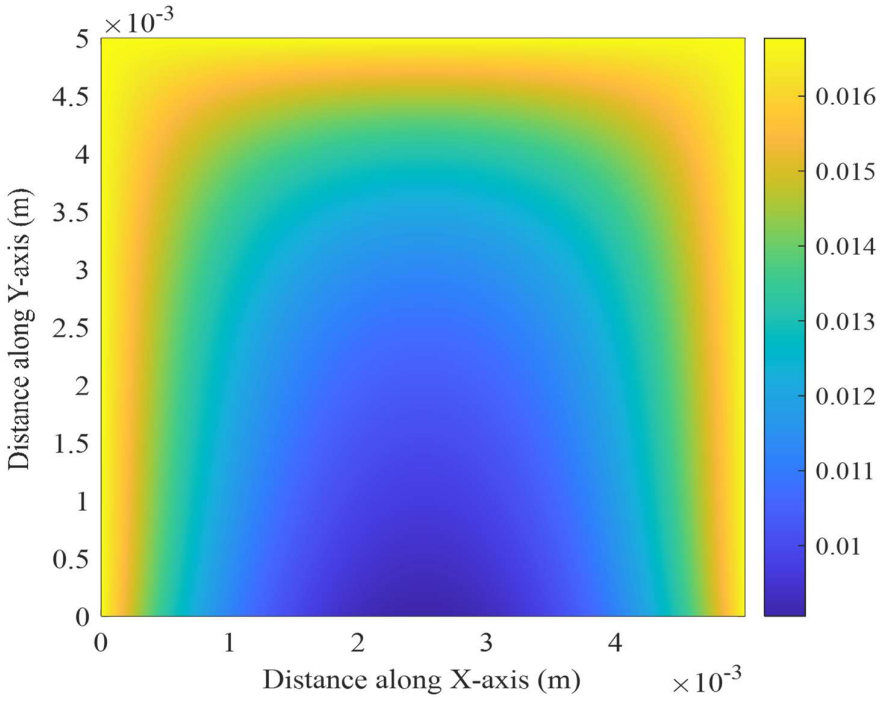
×10-3
5
4.5
4
3.5
3
2.5
2
1.5
1
0.5
0
Distance along Y-axis (m)
0
1
2
3
4
Distance along X-axis (m)
×10-3
0.016
0.015
0.014
0.013
0.012
0.011
0.01

(b)

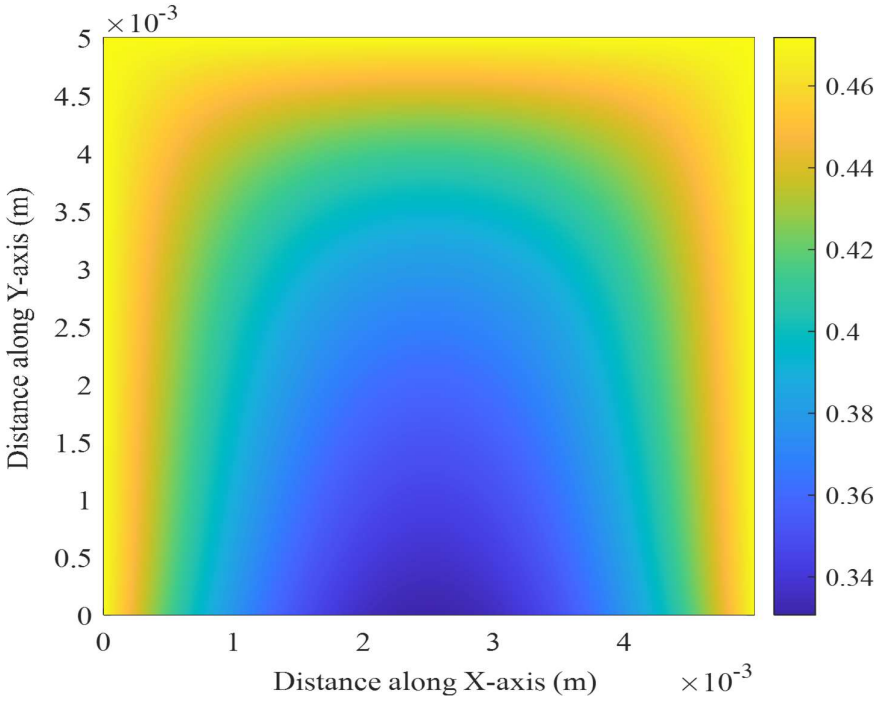

(c)

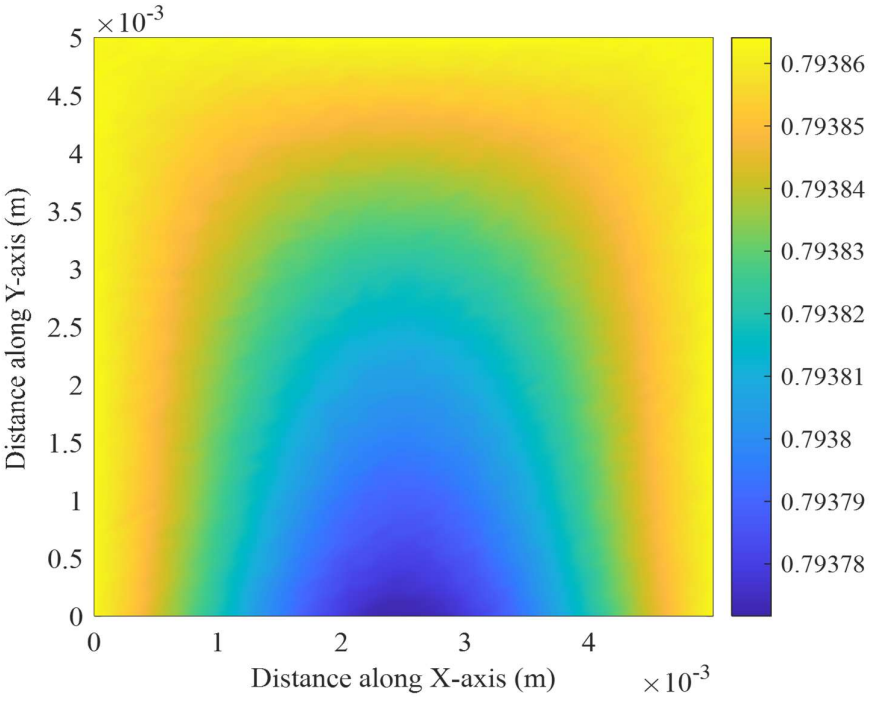

(d)

Figure 3.6: Distribution of ferrite at different times: **(a)** t = 5497s, **(b)** t = 5520s, **(c)** t = 5550s, and **(d)** t = 5580s

3.3.2 Validation of the predicted transformed phases with an existing literature (Karmakar *et al.* [104]) for cooling rate of 3.33 °C/s

Referring to the reported research paper by Karmakar *et al*. [104], the thermo-physical properties (Table. 2.3, Chapter-II, Section-2.2, sub-section 2.2.1) and the boundary conditions (Chapter-II, Section-2.3, sub-section 2.3.1) along with heating-cooling condition (Fig. 2.2, Table. 2.1, Chapter-II, Section-2.2) are set accordingly in the developed FORTRAN code. Respective prediction of the temperature distribution, cooling rate distribution, and evolution of the phases are discussed previous section (3.3.1). The final fractions of transformation for all the phases are presented in the Table. 3.3 (column 2 and 3) along with the time of transformation (column 1). The corresponding fractions of transformation reported by Karmakar *et al*. [104] based on experimental investigation, are presented in the column 4 of Table. 3.3. It is found that percentage of ferrite transformation agreed well with the numerical prediction. Karmakar *et al*. [104], instead of considering the bainite individually, a mixture of bainite with other phases is considered, accordingly, a lower value in fraction of transformed bainite is obtained in the present work. The fraction obtained in the present work for the pearlite phase is almost similar to that of the experimental value presented by Karmakar *et al*. [104]. Overall, a good agreement of the computational prediction is found with the experimental prediction.

Table 3.3: Phase transformation fractions at the cooling rate of 3.33 °C/s

Phases	***Transformation Time (s)***	***Transformed Fraction***	***Transformed (in %)***	***Comparison with Karmakar et al. [104]***
Ferrite	100	0.79	79	79
Bainite	15	0.048	4.8	10
Pearlite	33	0.16	16	11

3.4 Parametric Study

In the present work, a parametric study is also conducted for understanding the effect of process parameters on solid phase transformation of plain C-Mn steel. Out of many process parameters, the major process parameter involved in the process of solid phase transformation is the variation of cooling rate and concerned temperature of phase transformation. Accordingly, the present study is extended under different cooling rate conditions. Based on the considered cooling rate and related transformation temperature, the CCT diagram of the plain C-Mn steel is modelled in order to identify the phases those are to be transformed under the applied conditions, lead to prediction of different phases.

In the present work, different cooling rates such as 2.7 ℃/s, 1.4 ℃/s, 1.36 ℃/s, 1.12 ℃/s, and 0.74 ℃/s are considered apart from the cooling rate of 3.33 ℃/s. Under these different cooling rate conditions, the developed FORTRAN code is extended for evolution of the phases and corresponding fraction of transformation using the CCT model and Avrami equation, respectively. Under different conditions, different fraction of transformed phases is obtained. The fraction of phases obtained under different cooling rate conditions are presented in the Table. 3.4.

As presented in the Table. 3.4, with decreasing cooling rate, the transformed fraction of ferrite remains almost same upto cooling rate of 2.7 ℃/s from 3.33 ℃/s. If the cooling rate decreases further (i.e., if CR < 2.7℃/s), the transformed fraction of ferrite increases with decreasing cooling rate. As the cooling rate decreases, the transformation period of ferrite increases as presented the column (4) of Table. 3.4, which results an increase in the ferrite phase. Further it is mentioned here that this transformation also depends on the temperature combinedly with the cooling rate condition.

In case of bainite, it is found that the fraction of transformation decreases (4.8-0.2 as presented in the Table. 3.4) with a decrease in cooling rate. As the cooling rate decreases, the transformation period of bainite increases as presented the column (7) of Table. 3.4. In case of bainite, with decrease in cooling rate, the domain of bainite transformation decreases as presented in the CCT diagram (Fig. 2.3).

In case of pearlite, the fraction of transformation increases with decrease of cooling rate initially due to increase in transformation time at moderate temperature, and with further decrease in cooling rate, the transformation temperature is high that allows a decrease in

fraction of transformation following the CCT diagram (Fig. 2.3). As the cooling rate decreases, the transformation period of pearlite increases as presented the column (10) of Table. 3.4.

The obtained transformed fraction of phases is then compared with experimental prediction by Karmakar *et al*. [104]. A good agreement is found in case of ferrite phase. In case of bainite, comparatively a lesser value is obtained as a mixture of bainite with other phases is considered in case of the prediction by Karmakar *et al*. [104]. Accordingly, a higher value is obtained in case of pearlite compared to the prediction by Karmakar *et al*. [104]. The overall comparison of all the phases is presented in the Fig. 3.7, which shows a good agreement with the experimental prediction.

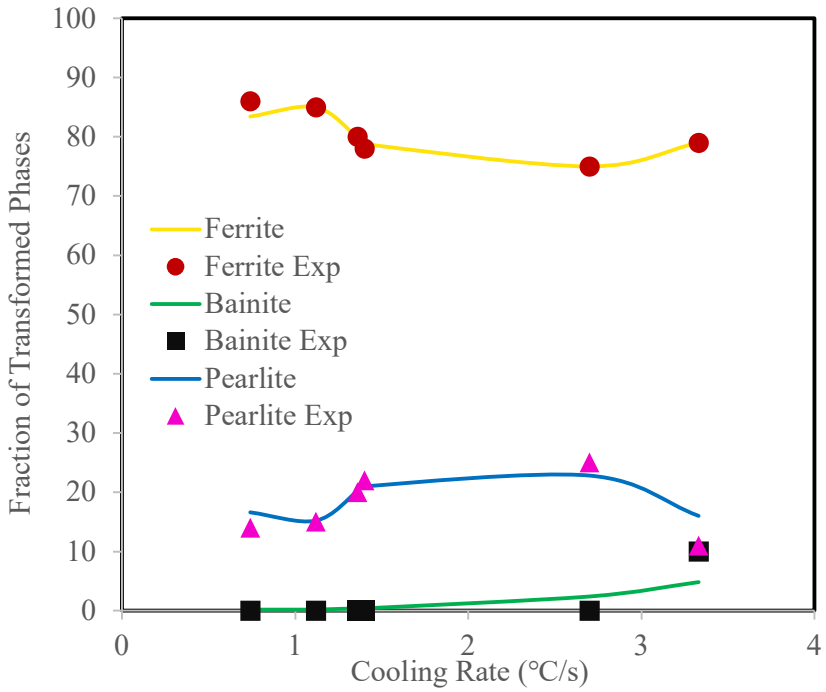

Figure 3.7: Comparison of the numerical prediction with experimental prediction by Karmakar *et al*. [104]

3.5 Closure

In the present chapter, evolution of transformation of all the phases in solid state is presented under different cooling rate conditions. All the prediction is compared with an existing experimental prediction by Karmakar *et al*. [104]. A good agreement in the numerical prediction is found compared to the experimental prediction.

Table 3.4: Fraction of transformed phases for different cooling rates and their transformation times

Cooling Rate (°C/s)	*Ferrite*			*Bainite*			*Pearlite*		
	Present Prediction (%)	*Karmakar et al., 2017*	*Transformation Time (s)*	*Present Prediction (%)*	*Karmakar et al., 2017*	*Transformation Time (s)*	*Present Prediction (%)*	*Karmakar et al., 2017*	*Transformation Time (s)*
3.33	79	79	100	4.8	10	15	16	11	33
2.7	75	75	124	2.4	-	16	22.8	25	45
1.4	78.8	78	245	0.4	-	24	21	22	101
1.36	79.8	80	252	0.4	-	25	20.2	20	104
1.12	85	85	307	0.2	-	28	15.2	15	132
0.74	83.4	86	469	0.2	-	34	16.6	14	201

References

[104]. A. Karmakar, P. Sahu, S. Neogy, D. Chakrabarti, R. Mitra, S. Mukherjee, and S. Kundu, Effect of Cooling Rate and Chemical Composition on Microstructure and Properties of Naturally Cooled Vanadium-Microalloyed Steels, *Metallurgical and Materials Transactions A*, Vol. 48, 2017, pp. 1581-1595

CHAPTER – IV

Conclusion and Future Scope of the Work

4.1 Conclusion

Researchers from all over the world are very interested in the study of solid phase transformation using a computational method that involves mathematical and numerical modeling because of its numerous and growing applications in engineering. Additionally, the innovation of materials has grown in recent decades, with steel leading in this regard due to its vast range of uses in all technical sectors and superior qualities over other materials. These steel characteristics are dependent on the phases that change when the material cools. In this regard, a number of studies on solid phase transformation that are referred in the literature mostly focus on experimental investigations. In reality, controlling the steel's characteristics requires a real-time prediction of this phase change, which is challenging to achieve through experimental procedures. Moreover, experimentation is very costly. This work, therefore, includes a numerical study on solid phase transformation of a plain C-Mn steel.

Accordingly, this work considers a suitable problem referring to the furnace of heating, holding, and cooling of the plain C-Mn steel. Suitable boundary conditions are then considered to represent the cooling behaviour of the steel, phase transformation phenomena and evolution of the fraction of phases depending on the heating condition, holding time, and cooling condition of the material. Then a suitable mathematical model to represent the heating and cooling process, is considered using the energy equation along with a volumetric source term representing evolution of heat due to phase transformation. The major challenge in this work is the identification of phases to be transformed during cooling of the steel. Thus, the continuous cooling transformation (CCT) diagram of the plain C-Mn steel obtained from JMatPro® software is modelled based on the cooling rate and transformation temperature those identify the phase/s of transformation. In the model, the phase transformation of the phases is considered using the Avrami equation, which allows to calculate the fraction of transformation. Along with the transformed fraction, this work also predicted the transformation time of each phase during cooling.

Subsequently, a numerical code in the FORTRAN platform is developed. The numerical code is developed based on the finite volume method (FVM) considering the Crank-Nicolson scheme for discretizing the governing equations. The subsequent solution of the finally obtained discretized simultaneous equations is performed on the basis of TDMA algorithm. Accordingly, the code is developed along with grid independent study. The developed code is then extended to predict the evolution of the phases during cooling of the plain C-Mn steel.

Thereby, the code is validated with a previously cited literature Karmakar *et al*. [104] and found a very good agreement. Since cooling rate is a major process parameter to control the transformation of the phases, the code is further extended and a parametric study is also included under different cooling rates.

The major findings using the present model of phase transformation include

1. identification of phases under transformation under different cooling rate conditions,
2. a real-time phase transformation of the plain C-Mn steel,
3. instantaneous distribution of the cooling rate, and subsequent control to the desired phases,
4. prediction of transformation time of any phase, and
5. prediction cost is very low compared to the experimental prediction, etc.

4.2 Future Scope of the Work

1. Other materials with different chemical composition can be used.
2. A range of cooling rates can be used to achieve the desired phases.
3. Transformation time can be utilised for controlling and saving prolonged exposure to cooling and heating cycles, thereby saving valuable time and resource.
4. Evolution of phases can be modified based on requirements and conditions.
5. The efficiency and the optimization of the transformation of phases at different cooling rates can be enhanced.
6. For more precise answers, improved performance, and accuracy, further numerical research can be done.